



HAL
open science

Large-scale diversity reassessment, evolutionary history, and taxonomic revision of the green macroalgae family Udoteaceae (Bryopsidales, Chlorophyta)

Laura Lagourgue, Claude Payri

► **To cite this version:**

Laura Lagourgue, Claude Payri. Large-scale diversity reassessment, evolutionary history, and taxonomic revision of the green macroalgae family Udoteaceae (Bryopsidales, Chlorophyta). *Journal of Systematics and Evolution*, In press, 10.1111/jse.12716 . hal-03232049

HAL Id: hal-03232049

<https://hal.sorbonne-universite.fr/hal-03232049>

Submitted on 21 May 2021

HAL is a multi-disciplinary open access archive for the deposit and dissemination of scientific research documents, whether they are published or not. The documents may come from teaching and research institutions in France or abroad, or from public or private research centers.

L'archive ouverte pluridisciplinaire **HAL**, est destinée au dépôt et à la diffusion de documents scientifiques de niveau recherche, publiés ou non, émanant des établissements d'enseignement et de recherche français ou étrangers, des laboratoires publics ou privés.

17 **Abstract:**

18 Udoteaceae is a morphologically diverse family of the order Bryopsidales. Despite being very
19 widespread geographically, this family is little known compared to the closely related Halimedaceae
20 or Caulerpáceae. Using the most extensive Udoteaceae collection to date and a multilocus genetic
21 dataset (*tufA*, *rbcL* and 18S rDNA), we reassessed the species diversity of the family, as well as the
22 phylogenetic relationships, the diagnostic morpho-anatomical characters and evolutionary history of
23 its genera, toward a proposed taxonomic revision. Our approach included a combination of
24 molecular and morphological criteria, including species delimitation methods, phylogenetic
25 reconstruction and mapping of trait evolution. We successfully delimited 62 species hypotheses, of
26 which 29 were assigned (existing) species names and 13 represent putative new species. Our results
27 also led us to revise the genera *Udotea* s.s., *Rhipidosiphon* s.s. and *Chlorodesmis* s.s., to validate the
28 genus *Rhipidodesmis* and to propose three new genera: *Glaukea* gen. nov., *Ventalia* gen. nov., and
29 *Udoteopsis* gen. nov. We also identified two large species complexes, which we refer to as the
30 “*Penicillus-Rhipidosiphon-Rhipocephalus-Udotea* complex” and the “*Poropsis-Penicillus-*
31 *Rhipidodesmis* complex”. Using a time-calibrated phylogeny, we estimated the origin of the family
32 Udoteaceae at Late Triassic (ca 216 Ma), whereas most of the genera originated during Paleogene.
33 Our morphological inference results indicated that the thallus of the Udoteaceae ancestor was likely
34 entirely corticated and calcified, composed of a creeping axis with a multisiphonous stipe and a
35 pluristromatic flabellate frond. The frond shape, cortication and calcification are still
36 symplesiomorphies for most extant Udoteaceae genera and represent useful diagnostic characters.

37 **Key words:** Chlorophyta; macroalgae; species delimitation; phylogeny; trait evolution

38 1.INTRODUCTION

39 Udoteaceae J. Agardh is a family of green siphonous macroalgae belonging to the order Bryopsidales
40 J. H. Schaffner. The family has a worldwide distribution with representatives occurring in tropical,
41 subtropical and temperate regions throughout the Atlantic, Indian and Pacific oceans as well as in the
42 Red Sea and the Mediterranean Sea. Udoteaceae species are most abundant in reef ecosystems
43 where they play an important ecological function as primary producers, contribute to carbonate
44 fluxes and provide shelter and food to other organisms (Goreau, 1963 ; Wray, 1977 ; Ries, 2006 ;
45 Payri, 2000 ; Granier, 2012). Currently, the family, which includes both calcified and non-calcified
46 taxa, accounts for eight extant genera and 64 species (Guiry & Guiry, 2020), if we exclude: 1)
47 synonymized or invalid genera (*Ancestria*, *Neseae*, *Coralliodendron*, *Corallocephalus*, *Espera* (syn. of
48 *Penicillus*); *Decaisnella* and *Geppina* (syn of. *Udotea*); *Flabellaria* J. V. Lamouroux (syn. of *Flabellia*);
49 *Rhipidodesmis* (syn. of *Chlorodesmis*); *Poropsis* Nizamuddin (uncertain) and *Flabellaria* Lamarck
50 (nom. illeg.) ; and 2) genera previously shown to be unrelated to the Udoteaceae (*e.g.*,
51 *Botryodesmis*, *Pseudochlorodesmis* and *Siphonogramen* (Verbruggen et al. 2009a); *Boodleopsis*,
52 *Callipsygma* and *Johnson-sea-linkia* (Cremen et al., 2019); *Chloroplegma* (syn. of *Avrainvillea*; Wade
53 et al 2018), *Rhipiliella* (probably belonging to Rhipiliaceae; Dragastan et al., 1997). A total of 20
54 species included in these genera can then be subtracted from the overall species diversity previously
55 included in the Udoteaceae.

56 Although they are all siphonous and composed of a unique giant and multinucleate tubular cell,
57 Udoteaceae genera are remarkable for their morphological diversity. Their forms range from
58 dichotomous filaments, single or grouped in tufts, to more complex thalli with characteristic frond
59 morphologies (*e.g.*, capitate for the genus *Penicillus* or flabellate for *Udotea*).

60 Since its publication by Agardh (1887), the most comprehensive work on Udoteaceae was published
61 by Gepp & Gepp (1911). Several authors have subsequently contributed to improving knowledge of
62 species diversity (Farghaly, 1980; Meinesz, 1980; Littler & Littler, 1990a and b; Vroom et al., 1998;

63 Collado-Vides et al., 2009), and with the discovery of new species and the increase in morphological
64 information, several authors have discussed the need to redefine genera (Agardh, 1887; Gepp &
65 Gepp, 1911; Nizamuddin, 1963; Farghaly, 1980; Littler & Littler, 1990a; Dragastan et al., 1997). The
66 few molecular-based studies conducted on Udoteaceae have highlighted conflicts between
67 morphological and molecular information, revealing polyphyletic genera (*i.e.*, *Chlorodesmis*,
68 *Penicillus*, *Poropsis*, *Rhipocephalus*, *Rhipidosipon* and *Udotea*) and unresolved phylogenetic
69 relationships for most taxa (Kooistra, 2002; Lam & Zechman, 2006; Curtis et al.; 2008; Verbruggen et
70 al., 2009a and b; Coppejans et al., 2011; Lagourgue et al., 2018; Wade & Sherwood, 2018; Cremen et
71 al., 2019). When reassessing the classification of the order Bryopsidales using the chloroplast
72 genome, and to avoid proliferation of new families with a parsimonious and practical purpose,
73 Cremen et al. (2019) proposed to abandon the Udoteaceae family in favor of tribe Udoteae, which
74 the authors placed in family Halimedaceae Link together with other families such as Rhipiliaceae
75 Kützing and Pseudocodiaceae L. Hillis-Colinvaux, and the genus *Halimeda*. However, we believe that
76 this decision overlooked morpho-anatomical variability and existing genera and species diversity in
77 the clade that we therefore prefer to maintain as the family Udoteaceae. Indeed, studies on closely
78 related families (Halimedaceae, Caulerpaceae Kützing) revealed unexpected species diversity
79 (Verbruggen et al., 2005a and b; Sauvage et al., 2013) and highlighted the existence of new lineages
80 at the family level with low morphological differentiation (Sauvage et al., 2016; Verbruggen et al.,
81 2017, Cremen et al., 2019). This contrasts sharply with the family Udoteaceae, whose rich species
82 and genus diversity remains to be reassessed. The genetic data available for Udoteaceae is
83 fragmentary (122 sequences for *tufA*, *rbcl* and 18S rDNA) and is limited to 26 of the current 64
84 species, often with only one sequenced marker per specimen and some level of misidentification.
85 Numerous tools have been developed to assess diversity and delimitate species that are now largely
86 applied across various macroalgal taxa. These include tree-based methods such as the General Mixed
87 Yule Coalescent (GMYC) (Pons et al., 2006) and its Bayesian implementation, bGMYC (Reid &
88 Carstens, 2012), the Poisson tree process model (PTP, Zhang et al., 2013) and the Multi-rate version,

89 mPTP (Kapli et al., 2017), as well as methods directly relying on genetic distances, such as the
90 Automatic Barcode Gap Discovery (ABGD, Puillandre et al., 2012a). For robust species hypothesis,
91 several authors have recommended to search for congruence between the different methods
92 applied to several genes (Carstens et al., 2013; Carstens & Knowles, 2007; Dupuis et al., 2012; Leliaert
93 et al., 2014; Puillandre et al., 2012b; Rannala, 2015) and to compare molecular-based partitions with
94 non-genetic data (Carstens et al., 2013; Carstens & Knowles, 2007; Fujita et al., 2012; Talavera et al.,
95 2013; Wiens, 2007).

96 Additionally, the large morphological diversity of Udoteaceae genera and species illustrates a
97 complex pattern of diversification within the Bryopsidales, which has led to several hypotheses on
98 the morphology of its ancestor (Gepp & Gepp, 1911; Littler & Littler, 1990a; Vroom et al., 1998;
99 Kooistra, 2002). To date, these hypotheses remain untested (*e.g.*, calcified or uncalcified ancestor),
100 and the family represents an original and interesting case study for an evolutionary approach.
101 Analytical methods, including statistics (Dubois, 2007; Rabosky et al., 2013) make it possible to
102 analyze the phylogenetic evolution of morphological characters and the genotype/phenotype
103 correlation by measuring, for example, the phylogenetic signal of morphological characters. The
104 phylogenetic inference of trait evolution is another relevant approach, which has been little used for
105 the study of macroalgae, with only three studies applied to green siphonous macroalgae (*Codium*
106 (Verbruggen et al., 2007); *Halimeda* (Verbruggen et al., 2009c) and *Pseudocodium* (Payri &
107 Verbruggen, 2009)). By using this approach, it is possible to explore the evolution of morpho-
108 anatomical characters both in time and across lineages and to test hypotheses about the ancestral
109 state of various characters. It is then possible to highlight relevant characters to discriminate groups
110 of species or specific morphological patterns, which together allow a better understanding of the
111 evolutionary history of the taxa studied. Phylogenetic inference of trait evolution is therefore of
112 particular interest, among others, for integrative taxonomy approaches based on data of various
113 origins (molecular, morphological, ecological, functional data, etc.) (Dayrat, 2005; Schlick-Steiner et
114 al., 2010; Garbino, 2018).

115 Using the largest Udoteaceae taxon sampling to date and a multilocus genetic dataset (*tufA*, *rbcl* and
116 18S rDNA), we aim to reassess the species diversity of the family, the phylogenetic relationships, the
117 diagnostic morpho-anatomical characters of its genera, as well as the morphological and
118 evolutionary history of the lineages, and to provide the necessary taxonomic revisions. To reach
119 these objectives, we use a combination of molecular and morphological approaches, including
120 species delimitation methods, phylogenetic reconstruction, time-calibrated analyses and inference
121 on the evolution of morpho-anatomical characters.

122

123 **2. Material and Methods**

124 **2.1 Sampling**

125 Samples were collected using SCUBA down 60 m deep or snorkeling from various localities worldwide
126 including in the Atlantic, Indian and Pacific oceans as well as the Red Sea and the Mediterranean Sea.
127 A total of 644 samples were processed in this study, including 527 samples collected by the authors
128 and 117 obtained through collaborations (Table S1 in Supporting Information). Vouchers were
129 pressed-dried on herbarium sheets and housed in various herbariums, including NOU in New
130 Caledonia, PC in France and GENT in Belgium (herbarium abbreviations follow Thiers (2019),
131 continuously updated). Subsamples of the fresh specimens were preserved in a 5% formaldehyde
132 solution in sea water for later morpho-anatomical observations and both in 95% ethanol and silica
133 gel for later DNA extractions.

134 **2.2 Morphological characters and analyses**

135 Morpho-anatomical observations were made on fragments preserved in formaldehyde or directly on
136 herbarium specimens. Calcified specimens were previously treated with a 5% hydrochloric acid
137 solution for 1 to 2 hours. Observations and measurements were made using an A2 Imager
138 microscope (Axio) fitted with a Canon EOS-100D camera. Photos of macroscopic characters were

139 made using a binocular microscope (Wild M3Z) equipped with a Canon EOS-700D camera. All
140 morpho-anatomical characters reported in previous studies were considered (Gepp & Gepp, 1911;
141 Littler & Littler, 1990a, b; Ducker, 1967; Coppejans et al., 2011). A selection of 30 discrete (10 binary
142 and 20 multivariate) and two continuous characters were analyzed, including morphological (*e.g.*,
143 thallus, stipe, frond shape, attachment type) and anatomical characters (*e.g.*, siphon diameter and
144 form, branching type, secondary structures). For each species, the different states of character were
145 encoded into a matrix without ordination or weight. All character states are synthesized in
146 Supporting Information (Data S1).

147 **2.3 DNA sequencing and alignment**

148 Samples were extracted using either the Plant mini Kit (Qiagen Inc, Valencia, CA, USA) (for
149 *Chlorodesmis*), the Blood and Tissue Kit (Qiagen Inc, Valencia, CA, USA) (for calcified genera, *i.e.*,
150 *Udotea*, *Penicillus*, *Rhipocephalus*, *Tydemania*) or the CTAB protocol (for *Rhipidosiphon* and *Poropsis*).
151 Two chloroplast markers were targeted, *tufA* and *rbcl*, as well as the 18S rDNA nuclear gene using
152 previously published primers (Händeler et al., 2010; Kooistra, 2002; Lam & Zechman, 2006;
153 Verbruggen et al., 2009b) (see Table S2). PCR reactions were conducted in a final volume of 25 μ L
154 including 12.5 μ L of AmpliTaq Gold 360 Master Mix (Applied Biosystems), 1 μ L of each primer (10
155 μ M), 0.75 μ L of dimethylsulfoxide (DMSO), 1 μ L of bovine serum albumin (BSA), 2.5 μ L of DNA and
156 6.25 μ L of ultra-pure water. PCR programs follow Lagourgue et al. (2018). The Sanger sequencing
157 reaction was carried out using 20 μ L of PCR product by Genoscreen (Lille, FRANCE). Sequences were
158 then edited in Geneious version 7.1.9 (<http://www.geneious.com>, Kearse et al., 2012) and aligned for
159 each marker separately using the MUSCLE algorithm available in the software. Sequences obtained
160 from collaborators and Genbank were added to our dataset. As far as possible, a maximum of
161 specimens from the type localities have been included in the analyses. When none was available,
162 Genbank sequences that did not come from the type localities were considered with caution for the
163 risk of misidentification by previous authors.

164 **2.4 Composition of the datasets**

165 The two chloroplasts markers, *tufA* and *rbcl*, known for their discriminatory power at the species
166 level in green macroalgae (Leliaert et al., 2014; Saunders & Kucera, 2010; Verbruggen et al., 2009b)
167 were selected for species delimitation analyses. Maximum Likelihood (ML) and Bayesian ultrametric
168 trees were reconstructed from single marker alignments, after removing identical haplotypes using
169 the Collapsetypes v4.6 perl script (Chesters, 2013). Outgroup taxa (see Table S3) were also removed
170 before running species delimitation analyses.

171 In addition, two different concatenated multilocus matrices (*tufA*, *rbcl* and 18S rDNA) were compiled
172 to perform phylogenetic analyses. The first was composed of several specimens per species, for
173 which at least two of the three markers were available, to assess the taxonomic position and
174 composition of the different Udoteaceae genera. The second dataset corresponded to a selection of
175 one specimen per species (as defined by the species delimitation approach) and was intended for
176 evolutionary analyses and time-calibrated phylogeny. A total of ten outgroup species were added to
177 the second dataset to ensure proper phylogenetic calibration (see Table S3).

178 **2.5 Tree inference**

179 Prior to the phylogenetic analyses, each dataset was analyzed with Partition Finder v1.1.0 (Lanfear et
180 al., 2012) to determine the best partition schemes and the most suitable evolutionary models based
181 on the Akaike information criterion (AIC). As the sequencing success was uneven between the two
182 parts of the *rbcl* gene, we chose to consider them separately (as *rbcl5'* and *rbcl3'*) to improve the
183 modelling.

184 For each dataset, ML trees were reconstructed using RAXML (Stamatakis, 2014) through the CIPRES
185 web portal (Miller et al., 2010). ML analyses were launched using the “rapid bootstrapping and
186 search for the best-scoring ML tree” algorithm, the GTR+I+G evolutionary model and 1,000 bootstrap
187 (bs) iterations (Stamatakis et al., 2008).

188 Bayesian ultrametric trees (for species delimitation analyses) were estimated using BEAST
189 (Drummond et al., 2012) through the CIPRES web portal. Two independent analyses of 30 and 40
190 million generations were run for *tufA* and *rbcl*, respectively, and sampled every 1,000 generations.
191 The Likelihood ratio test, using MEGA 6 (Tamura et al., 2013), rejected the null clock hypothesis;
192 trees were, therefore, estimated using a relaxed lognormal molecular clock (Drummond et al., 2006)
193 with a coalescent constant size tree prior as recommended by Monaghan et al. (2009).

194 The Bayesian inference (BI) on the multilocus matrix (*tufA*, *rbcl*, and 18S) composed of several
195 specimens per species, was performed using MrBayes v.3.2 (Ronquist & Huelsenbeck, 2003) through
196 the CIPRES portal. The analysis was carried out in two independent runs of four incrementally heated
197 chains of 50 million generations, sampled every 1,000 generations, with a burn-in set at 10 %.

198 The time-calibrated phylogeny was carried out using BEAST v.2.5.0 (Bouckaert et al., 2014) through
199 the CIPRES web portal. It was estimated under a Calibrated Yule model (Heled & Drummond, 2012)
200 and a relaxed lognormal molecular clock (Drummond et al., 2006). Two independent analyses were
201 run for 75 million generations and sampled every 10,000 generations.

202 For all Bayesian analyses, each run output was checked in Tracer v.1.5 (Rambaut & Drummond, 2007)
203 to confirm the convergence of the Markov Chains Monte Carlo (MCMC) and that effective sample
204 size (ESS) values were all above 200, before computing a consensus topology and posterior
205 probabilities. For Beast trees, the outputs were combined using Log Combiner (included in the BEAST
206 package), removing the first 10% generations as burn-in. The Maximum Clade Credibility Tree (MCCT)
207 was calculated using Tree Annotator (included in the BEAST package).

208 Outgroup taxa, partition schemes, evolutionary models, and reconstruction parameters for all ML
209 and BI trees are detailed in Table S3 (Supporting Information).

210 **2.6 Species delimitation methods**

211 Five species delimitation methods were used to assess the Udoteaceae species diversity based on the
212 chloroplast markers: ABGD, GMYC, bGMYC, PTP and mPTP. The species delimitation process then
213 consists of comparing the different primary species hypotheses (PSHs) resulting from the species
214 delimitation methods, and searching for congruence between the different markers analyzed to
215 define secondary species hypotheses (SSHs). In case of conflicts, a majority rule was applied, and the
216 most prevalent PSH was selected. Morpho-anatomical observations were then compared to
217 molecular-based species hypotheses to confirm SSHs, as well as to assign species names when
218 possible.

219 The ABGD method was applied to both *tufA* and *rbcl* alignments through the website:
220 <http://www.abi.snv.jussieu.fr/public/abgd/abgdweb.html>. The Kimura model (relative minimum gap
221 width (X) = 1) was used for the *tufA* analysis, while the JC (X = 0.5) and the SD models (X= 1) were
222 preferred for analysing the *rbcl*5' and *rbcl*3' fragments, respectively. All other parameters were used
223 with default values. GMYC was performed using the package "splits" in R (R Development Core Team,
224 2019) on bayesian MCCTs. The bGMYC method was applied using the "bGMYC" package (Reid &
225 Carstens, 2012) also in the R environment on a subsample of 100 BEAST trees. The analyses were
226 carried out on 10,000 and 15,000 MCMC generations, sampled every 100 generations, for *tufA* and
227 *rbcl*, respectively. The PTP method was conducted through the Exelixis Lab web server ([http://sco.h-](http://sco.hits.org/exelixis/web/software/PTP/index.html)
228 [its.org/exelixis/web/software/PTP/index.html](http://sco.hits.org/exelixis/web/software/PTP/index.html)) on the ML rooted tree and run for 500,000
229 generations for both *tufA* and *rbcl*, sampling every 1,000 generations and without considering the
230 outgroups. Finally, mPTP was carried out on the mPTP web server (<http://mPTP.hits.org>) both on
231 bayesian MCCTs and ML rooted tree with default settings for all parameters.

232 **2.7 Time calibration points**

233 For reconstruction of the time-calibrated phylogeny, three calibration points derived from fossil
234 information were used (Table S4): 1) *Halimeda soltanesis* - 250 million of years (Ma) (Poncet, 1989),
235 2) *Caulerpa* sp. - 280 Ma (Gustavson & Delevoryas, 1992), and 3) *Pseudopenicillus aegaeicus* - Late

236 Triassic (Dragastan et al., 1997). Due to the lack of convergence of runs and low ESS values during
237 preliminary analyses, likely because of bias in paleontological dating and/or erroneous phylogenetic
238 placement, we choose not to consider the age of the fossil *Udotea palmetta* (Fiore, 1936). These
239 calibration points were set with uniform distributions and minimal age corresponding to the
240 estimated age of the fossil (*cf.* Table S4). Three additional calibration points were selected from the
241 study of Verbruggen et al. (2009b): 1) Bryopsidales root – 456 Ma, 2) Crown of Core Halimedineae –
242 391 Ma, and 3) Crown of Halimedaceae + Pseudocodiaceae + Udoteaceae – 273 Ma. They were
243 constrained using corresponding ages and normal distributions (*cf.* Table S4 for more details).

244 **2.8 Phylogenetic signal and correlation analyses**

245 The phylogenetic signal is based on the assumption that phylogenetically related organisms tend to
246 resemble each other phenotypically. In this study, the phylogenetic signal was measured to identify
247 whether a morphological trait followed this trend or appeared more labile and unpredictable. Our
248 aim was to assess the relevance of each trait to provide revised morphological descriptions. For the
249 continuous characters, the phylogenetic signal (PS) was estimated with Blomberg's K (Blomberg et
250 al., 2003) and Pagel's λ (Pagel, 1999) statistics using the "phylosig" function of the phytools package
251 (Revell, 2012) in R. These two measures quantify trait variation with respect to the "random walk"
252 model of the Brownian motion (BM). If $K=1$, the PS is strong and in accordance with the BM model; if
253 $K<1$, the PS is lower than under the BM model; if $K=0$, there is no PS (the trait evolves independently
254 of the phylogeny); if $K>1$, the PS is stronger than expected under the BM model (close species are
255 more similar than expected under the BM). If λ equals or is close to 0, there is no PS; if $\lambda=1$, the PS is
256 strong (the trait evolves following the BM model); if $0<\lambda<1$, a PS exists, but the trait does not evolve
257 according to the BM model and probably follows another process (*e.g.*, Ornstein-Uhlenbeck, OU).
258 The evolutionary model best adapted to the trait evolution (BM, OU or the "early-bust" model) was
259 tested using the "geiger" package (Harmon et al., 2008). For discrete characters, the PS was
260 estimated with the phylogenetic D statistic (Fritz & Purvis, 2010) using the function "phylo.d" of the

261 “caper” package (Orme et al., 2013) in R. The D statistic calculates the ratio between the sum of the
262 sister clade differences, from which the BM expectation is extracted, and the difference between a
263 random estimate and the BM expectation. If $D < 0$, the trait has a strong PS; if $D > 0$, the trait has a PS
264 lower than expected with the BM model.

265 The correlation between discrete characters was computed using the function “fitpagel” of the
266 “phytools” package (Revell, 2012). For continuous characters, the phylogenetic generalized least
267 squares (PGLS) was calculated with the “nmls” package.

268 Multivariate discrete characters were converted to binary for estimating the D statistic (PS) and
269 Pagel’s test of correlation (see Data S1 for transformation).

270 **2.9 Ancestral states reconstruction**

271 To infer trait evolution on the phylogeny, we used the time-calibrated phylogeny of the family
272 reconstructed from the concatenated multilocus matrix and the characters matrix produced from the
273 morpho-anatomical observations. Ancestral state estimations were computed using the “phytools”
274 package (Revell, 2012). The “contMap” function was used for the continuous characters, while
275 estimations for discrete (binary and multivariate) characters were calculated using the
276 “make.simmap” function with 1,000 simulations. Equal probability was applied to each state of
277 character that was either missing or had a non-applicable (N.A.) value.

278 Based on the combination of molecular and morpho-anatomical data and using a likelihood criterion
279 and a defined number of iterations, these analyses reconstruct the ancestral state estimated at each
280 node for each character selected. The ancestral state estimation, therefore, represents the
281 probability of the different states of a given character at each node of the tree. This allows
282 identifying the status and taxonomic relevance of the morphological characters studied.

283 Synapomorphies (*i.e.*, derived states shared by at least two taxa and inherited from a common
284 ancestor) are useful in the taxonomic review process at genus-level and for documenting diagnoses.

285 Homoplasies (*i.e.*, similar states of character found between different species, which do not originate

286 from the same ancestor) cannot be used for species diagnoses, but provide information on the
287 evolutionary history of a particular trait and allow to explore its evolutionary pattern.

288 3. RESULTS

289 3.1 Genetic variability

290 A total of 1,056 sequences were obtained in this study, including 518 *tufA* sequences (852 base pairs,
291 bp), 397 *rbcl* sequences (1,365 bp-long, including 763 bp of the *rbcl5'* fragment and 602 bp of the
292 *rbcl3'* fragment), and 141 18S rDNA sequences (1,226 bp). The *tufA* dataset had 179 unique
293 haplotypes and 482 variables sites (57.24 %). The *rbcl* dataset had 139 unique haplotypes and 496
294 variables sites (36.3 %), with the *rbcl5'* and *rbcl3'* fragments accounting for 287 (37.61%) and 209
295 variable sites (34.72%), respectively. Finally, the 18S rDNA dataset had 222 variables sites (18.10%).
296 From our dataset, *tufA* appeared more variable than *rbcl*. The *rbcl5'* fragment was more variable
297 than the *rbcl3'* fragment, which corroborates the results of Lagourgue et al. (2018) for the Caribbean
298 Udoteaceae species, and contrasts with other studies on Bryopsidales families, for which the *rbcl3'*
299 fragment appeared more variable and informative than *rbcl5'* (Saunders & Kucera, 2010).

300 A total of 422 sequences have been submitted to the Genbank under accession numbers MT324398-
301 MT324484 for 18S rDNA sequences, MT339592-MT339713 and MT456567-MT456591 for *rbcl*
302 sequences and MT340305-MT340496 for *tufA* sequences (see Table S1).

303 3.2 Species delimitation and name assignment

304 **3.2.1 Primary Species Hypotheses (PSHs):** Results obtained with the five delimitation methods for
305 the *tufA* and *rbcl* datasets are summarized in Table 1 and are available in more detail in Supporting
306 Information (Figures S1 & S2 and Data S2). The PSHs support values of the hPTP method and the α
307 *posteriori* probabilities (PP) of bGMYC partitions are also given in Supporting Information (Data S3 &
308 S4 and Tables S5 & S6, respectively). The five methods recovered between 39 and 53 PSHs for *tufA*,
309 and between 48 and 56 PSHs for *rbcl*. Among those, a total of 23 and 35 PSHs were shared between

310 the five methods for *tufA* and *rbcl*, respectively. Several incongruences were found between the five
311 methods results for *tufA* as well as for *rbcl* (Figures S1 and S2 respectively). For the *tufA* dataset,
312 most discrepancy was found for the delimitation of *Udotea* spp. (clades 24 to 29 and clades 38 & 39)
313 and *Chlorodesmis* spp. (clades 17 & 59) (Fig. S1). Similarly, for the *rbcl* dataset, most incongruences
314 were also found for delimitating some *Udotea* spp. (clades 26 to 29) and *Chlorodesmis* species
315 (clades 17, 21,22 and 59) (Fig. S2). For both markers, the GMYC and bMGYC methods were the most
316 conservative, whereas hPTP tended to over-split clades.

317 **3.2.2 Secondary Species Hypotheses (SSHs) and assignment:** Based on the common PSHs of the five
318 species delimitation methods (see Table S7) or the majority rule, a total of 50 and 54 SSHs were
319 retained for *tufA* and *rbcl*, respectively, out of which 42 SSHs were common between the two
320 markers. Most of them (24) were congruent between markers and with morpho-anatomical
321 observations and were, therefore, retained as valid species hypotheses. Some of the remaining SSHs,
322 which were not congruent between markers, were resolved using morpho-anatomical observations
323 (15), while others require further data and analysis (3). Table S8 (Supporting Information) provides
324 details on the incongruence resolution process, conclusions and species assignment.

325 Altogether, 62 SSHs were retained for the two markers combined. Among these, 29 SSHs were
326 identified to species level, five SSHs still require confirmation, and 13 SSHs could represent species
327 new to science. Another 15 SSHs were represented by sequences downloaded from the Genbank or
328 provided by collaborators, for which morpho-anatomical data were unavailable to confirm species
329 name assignment. Genera and species name assigned to the different SSHs are detailed in the
330 Supporting Information (Figures S1 & S2, Table S1).

331 **3.3. Phylogenetic relationships and evolution**

332 Our concatenated multilocus matrix (3,443 bp) included sequences for a total of 145 specimens,
333 which represented 43 genetically delimited species from several localities around the world from
334 which specimens had never been sequenced. The ML and BI phylogenies resulting from our analyses

(Fig. 1) provide new insights into the phylogenetic relationships of Udoteaceae taxa. They produced a total of ten well supported “terminal” clades corresponding to five Udoteaceae genera recorded as current taxonomically by Guiry & Guiry (2020) (*i.e.*, *Udotea*, *Rhipidosiphon*, *Chlorodesmis*, *Tydemanina*, *Flabellia*). Our results confirmed the polyphyly and paraphyly of the genera *Udotea*, *Chlorodesmis*, *Rhipidosiphon*, *Rhipocephalus*, and *Penicillus* as already pointed out in previous studies (Kooistra, 2002; Lam & Zechman, 2006; Curtis et al., 2008; Verbruggen et al., 2009a and b; Coppejans et al., 2011; Lagourgue et al., 2018; Wade & Sherwood, 2018; Cremen et al., 2019). Only *Tydemanina* and the monospecific genus *Flabellia* were monophyletic. The genus *Poropsis* is represented by only one species in this multilocus phylogeny, therefore we could not confirm its monophyly (but see the multiples *Poropsis* lineages retrieved in gene trees used for species delimitation analyses (Fig. S1 & S2), and which do not form a monophyletic clade). Although similar conclusions were reported in the literature previously, limited data and unresolved phylogenetic relationships prevented the authors from drawing taxonomic conclusions (Kooistra, 2002, Curtis et al., 2008, Lam & Zechman, 2006; Verbruggen et al., 2009b, Lagourgue et al., 2018). In our analyses, the family Udoteaceae was monophyletic (as defined in the introduction) with high node support (bs: 93; PP: 1) (Figure 1.A). This result contrasts with previous studies where *Tydemanina* was more closely related to Pseudocodiaceae than Udoteaceae (Verbruggen et al., 2009b; Sauvage et al., 2016) but corroborates the results of Cremen et al. (2019) (see nevertheless the differences between the chloroplast genes tree (*tufA* and *rbcL*) (Figures S3) which is similar to the concatenated multilocus topology (Fig. 1), and the nuclear 18S rDNA gene tree (Figure S4), where Udoteaceae is not monophyletic (*Tydemanina* and *Flabellia* branch with *Pseudocodium* species, although not supported). Here, using node support, the phylogenetic position of type species, the congruence of morphological characters, original diagnoses, published observations and/or proposals, as well as the ancestral character reconstruction, we selected nine clades (A-I, collapsed in Figure 1.B) on which we based our taxonomic revision proposal. Our findings led us to consider clades A, B, D and F, which contained type species for *Tydemanina*, *Udotea*, *Chlorodesmis* and *Rhipidosiphon*, respectively, as

361 representatives of current genera, for which we propose to redefine the taxonomic boundaries. Our
362 data also indicate that clades C, E, and G represent lineages requiring the establishment of new
363 genera (*Glaukea* gen. nov., *Ventalia* gen. nov. and *Udoteopsis* gen. nov., respectively), while the
364 taxonomic status of clades H and I (the “*Penicillus-Rhipidosiphon-Rhipocephalus-Udotea* (PRRU)
365 complex” and the “*Poropsis-Penicillus-Rhipidodesmis* (PPR) complex”, respectively) remains unclear
366 (see further below for discussion and diagnoses).

367 The time-calibrated phylogeny of the family Udoteaceae was reconstructed from the concatenated
368 multilocus matrix (*tufA*, *rbcl* and 18S rDNA) and results are shown in Figure 2. This tree is similar to
369 that shown in Figure 1 and node support is higher for the Bayesian inference than the maximum
370 likelihood method. The revised and new genera (*Chlorodesmis* s.s., *Rhipidosiphon* s.s., *Udotea* s.s.,
371 *Glaukea* gen. nov., *Ventalia* gen. nov. and *Udoteopsis* gen. nov.) were all monophyletic with strong
372 node support (bs > 90; PP >0.98) (but see the nuclear tree, where *Rhipidosiphon* is polyphyletic; Fig
373 S4)). Results indicate a divergence between the families Halimedaceae and
374 Pseudocodiaceae/Udoteaceae around 288 Ma (Permian, Paleozoic), while the divergence between
375 the families Pseudocodiaceae and Udoteaceae is around 246 Ma (Late Triassic, Mesozoic). The origin
376 of the Udoteaceae is estimated at about 216 Ma (Late Triassic), but its diversification began around
377 109 Ma (Early Cretaceous). The most recent speciation event is dated at 3.5 Ma, but most of the
378 extant species originated from diversification events during the Cenozoic (from ca 59 Ma) (Figure 2).

379 **3.4. Phylogenetic signal, correlation and ancestral reconstructions of morpho-anatomical** 380 **characters**

381 The analysis of morphological characters according to the phylogeny and the ancestral
382 reconstructions allowed us to understand the ancestral character states better and to identify those
383 relevant for our taxonomic proposal and revision.

384 Analysis of the phylogenetic signal for the two continuous traits by the Pagel’s λ test indicated the
385 presence of a strong phylogenetic signal following a BM model for the stipe siphon diameter and a

386 phylogenetic signal according to a model other than a BM for the frond siphon diameter (Tables S9).
387 The Blomberg's K test also found a phylogenetic signal for both traits, but weaker than in a BM model
388 (Table S9). Of the 27 discrete characters, 17 had a phylogenetic signal (Table S10), while 10 had no or
389 weak phylogenetic signal. The highest scores (D statistics) were found for: growth mode, type of
390 constrictions and absence or presence of a stipe (-2.05, -1.25 and -0.96, respectively); the lowest PS
391 values were found for: stipe ramification (1.04), type of dichotomies (1.36) and stipe siphon aspect
392 (1.79). Overall, the phylogenetic signal analyses revealed strong correlations with the phylogeny for
393 the majority of characters studied. Still, several of those traditionally used to distinguish between
394 Udoteae genera had a weak PS, including stipe shape, frond composition, branching pattern, siphon
395 aspect, type of dichotomy and presence or absence of constrictions. On the other hand, the external
396 habit or the type of constriction, which are characters rarely considered, appeared remarkable for
397 their strong phylogenetic signal. Similarly, calcification and thallus cortication also had strong PS,
398 which confirms their taxonomic relevance for the classification of Udoteaceae genera.

399 Our analyses of trait correlations also provided several interesting results which are detailed in Table
400 S11 and Data S5 (Supporting Information).

401 Finally, the ancestral state reconstruction results are provided in Supporting Information (Data S5)
402 with a summary of correlated characters, ancestral state estimation and the putative
403 synapomorphies, symplesiomorphies or homoplasies. Table 2 reports the results for discrete
404 characters that are the most relevant because 1) they show a PS; 2) the ancestral state could be
405 estimated for the Udoteaceae ancestor; and 3) homoplasies, synapomorphies or symplesiomorphies
406 could be identified (see Table S12 for these results for all the characters studied). Figure 3 presents
407 ancestral state reconstruction of four characters, that we consider the most important for
408 understanding the evolution of the Udoteaceae and revising the taxonomy of its genera. Frond shape
409 (Fig.3. A), thallus cortication (Fig 3.B), presence or absence of calcification (Fig. 3.C) and secondary
410 structures on frond siphons (Fig. 3.D) (all other characters are presented in Data S5).

411 The ancestral state (plesiomorphic) was identified for a total of 26 characters (Table S12). We also
412 found several homoplasies (convergent or parallel), as well as cases of regression or
413 synapomorphies, providing important information on the evolutionary trajectories of the different
414 characters. Additionally, we found that several characters states traditionally referenced in genus
415 diagnoses appeared to represent varying degrees of homoplasy. This is particularly true for the
416 presence of pores on the calcified surface of siphons (*e.g.*, *Rhipidosiphon s.s.*, *Penicillus*, *Poropsis*),
417 the alignment of dichotomies (*Rhipidosiphon*), the capitate frond of "*Penicillus*" (Figure 3.A), or some
418 characters used to identify species such as the branching of the stipe (*e.g.*, *Flabellia petiolata*, *Udotea*
419 *dixonii*, etc.), and the presence of descending lateral siphons (*Udotea glaucescens*, *R.*
420 *lewmanomontiae*) (Data S5). Our results also reveal, for the first time, that many states of character,
421 which used to be considered relevant and diagnostic of genera in previous Bryopsidales studies (*e.g.*,
422 the flabellate form, the presence of a stipe, total cortication, or total calcification) actually represent
423 symplesiomorphies within the family Udoteaceae (*i.e.*, states inherited from the family's ancestor
424 and maintained throughout evolution) (Fig. 3. A. to D and Data S5). The presence of these ancestral
425 states (plesiomorphic) is contrasted between genera, but they often still represent the majority of
426 the states observed. The most symplesiomorphic genera are *Flabellia*, *Udotea s. s.* and *Glaukea* gen.
427 nov. Conversely, the genera with the most derived states (homoplasies and synapomorphies) are
428 *Tydemania*, *Chlorodesmis s.s.* and *Rhipidodesmis s.s.*

429 All major findings for taxonomical purpose are reported for each genus in the following sections (4.3)
430 and corresponding figures (see Figures 4, 6, 7 and 9) and are also discussed in sections 4.2.1 to 4.2.5.

431

432 **4. DISCUSSION**

433 **4.1. Udoteaceae phylogenic evolution and diversity**

434 The topology of the time-calibrated phylogeny (Figure 2), based on one representative per species,
435 appeared similar to our comprehensive ML phylogeny (Fig. 1) and the proposed revised genera were

436 all monophyletic with strong node support (bs > 90; PP> 0.98). According to our results, the origin of
437 Udoteaceae dates back to about 216 Ma (Late Triassic), which corroborates the work of Verbruggen
438 et al. (2009b) and the calibration points used for the reconstruction. The divergence between the
439 families Halimedaceae and Udoteaceae/Pseudocodiaceae is estimated to about 288 Ma, which
440 corresponds to the Permian (Paleozoic) and Udoteaceae latter diverged from Pseudocodiaceae
441 during the Late Triassic (ca 246 Ma, Mesozoic). Most of the Udoteaceae genera originated during the
442 Paleogene (*i.e.*, between ca 66 and 23 Ma) and the most recent speciation event was estimated
443 around 3.5 Ma (Figure 2).

444 Our results also shown that for taxa of the family Udoteaceae, *tufA* and *rbcL5'* alone appear sufficient
445 to assess the variability at species-level and can be used as "barcodes". However, for a larger genetic
446 or phylogenetic analysis (several families or the order Bryopsidales), we recommend using *tufA*, and
447 the whole *rbcL* marker (or the *rbcL3'* fragment instead of the *rbcL5'*) so that results can be compared
448 to previous studies. In contrast, the 18S rDNA was less variable than the chloroplast markers and,
449 therefore, does not represent a good choice for species delimitation analyses.

450 Our results also demonstrate that the family Udoteaceae has high morphological complexity and
451 large species diversity, although this is not homogeneous across clades. Kooistra (2002) had already
452 pointed out to different genetic and morphological patterns within the family Udoteaceae with: 1)
453 fully corticated taxa being morphologically similar ("poor" in diversity), and corresponding to older
454 lineages with slower phenotypic diversification; and 2) uncorticated genera showing rapid
455 cladogenesis with considerable phenotypic changes between related species. This latter case of
456 diversification is found mainly in the "PRRU complex". The complex is monophyletic and
457 geographically restricted. However, it has many homoplasies with other taxa outside the clade that
458 are geographically disconnected, which illustrates parallel genetic and morphological evolutions. The
459 large morphological diversity of the Udoteaceae could thus be interpreted as a phenotypic

460 evolvability (*i.e.*, the ability of lineages to evolve with the production of morphological and ecological
461 novelties) that promotes speciation (Pigliucci, 2008; Adamowicz et al., 2008).

462 Finally, the analysis of the evolutionary history of the Udoteaceae provides a better understanding of
463 its very significant diversity, both in terms of species and genera, which has long been
464 underestimated but which is demonstrated here, through our results. Although there is no family or
465 tribe concept that is commonly accepted, we question the need for the revisions proposed by
466 Cremen et al. (2019), where such a species and genus rich family as Udoteaceae was downgraded to
467 tribe. Ultimately, whether one prefers Udoteaceae or Udoteae should not jeopardize the following
468 proposed taxonomic revision of the genera.

469

470 **4.2. Morphological evolution**

471 Through phylogenetic signal and correlation analyses, as well as the inference of morpho-anatomical
472 trait evolution on phylogenies, seven characters appeared as the most relevant for taxonomic
473 purposes as well as for the macroevolutionary models they represent. These characters (and their
474 most relevant states) are: the frond shape (particularly the “flabellate”, “capitate” and “caespitose”
475 states) (Fig.3. A.), the thallus cortication (particularly the “total thallus cortication” state) (Fig. 3. B),
476 the presence or absence of calcification (both states) (Fig. 3. C), the presence or absence of stipe
477 (both states), the presence or absence of pores on calcified siphons sheath (both states), the
478 secondary structures on frond siphons (particularly the “appendages” state) (Fig. 3. D) and, finally,
479 the type of supra-dichotomial constrictions (the “symmetrical” and “asymmetrical” states).

480 In the following sections, we use these characters and other results of our study to discuss various
481 hypotheses about the evolution of the family Udoteaceae.

482 **4.2.1 What did the Udoteaceae ancestor look like?** According to our results (*cf.* Data S5), the

483 Udoteaceae ancestor may have had a creeping axis with a multisiphonous non-ramified stipe and a

484 single pluristromatic flabellate frond (Fig. 3. A), all continuously joined together. It may have been
485 entirely corticated (stipe and frond) (Fig. 3. B) and calcified (Fig. 3. C), but the siphons' sheath may
486 have been non-porous. The siphons' ramifications may have been dichotomous and arranged in a
487 single plan, with unaligned isomorphic dichotomies and asymmetric supra-dichotomial constrictions.
488 Frond and stipe siphons may have been parallel to subparallel and may have had appendages (Fig. 3.
489 D). We estimated the average diameters of the frond and stipe siphons to be 95 μm and 70 μm ,
490 respectively. We have no precise estimation for the attachment system.

491 This ancestral morphology is close to the description of the fossil genus *Pseudoudotea* (calcified,
492 flabellate frond and siphons with "finger-like" appendages at the margin) described by Dragastan et
493 al. (1997). *Pseudoudotea* belongs to the family Pseudoudoteaceae, with other fossil genera such as
494 *Hydra* or *Garwoodia*. Missing information, such as the attachment system or stipe morphology,
495 makes a thorough comparison of their morphology with that of the putative Udoteaceae ancestor
496 impossible, but our results suggest that the morphological characters shared by *Pseudoudotea* and
497 the putative Udoteaceae ancestor could be the inheritance of a common ancestor between the two
498 families.

499 Dragastan et al. (1997) proposed to consider the fossil *Pseudopenicillus aegaeicus* as representative
500 of the former family Udoteaceae. The external morphology of the fossil is similar to the extant genus
501 *Penicillus*, with a stipe whose siphons bear dichotomously branched "secondary siphons"
502 (appendages) and a capitulum with free siphons. Although the age of the fossil (Early Triassic)
503 coincides with the temporal origin of the putative Udoteaceae ancestor, most of the fossil's
504 morphological characters differ from those inferred for the putative Udoteaceae ancestor. Based on
505 these observations, we believe that *Pseudopenicillus* represents an extinct genus of family
506 Udoteaceae and does not represent the most recent common ancestor of the entire family.

507 **4.2.2 Is the modern form inherited from a simple or a complex morphology?** Various hypotheses
508 have been put forward regarding the morphology of the most recent Udoteaceae ancestor. Some

509 authors argue for a simple, filamentous and uniaxial primitive form (Hillis-Colinvaux, 1984, Meinesz,
510 1980) or an uncorticated frond (Littler & Littler, 1999; Dragastan et al., 1997) from which genera with
511 more complex morphologies may have evolved through successive acquisitions of derived states.
512 Others prefer a complex ancestral form from which simpler forms may have emerged through
513 successive secondary losses of character states (Kooistra, 2002; Verbruggen et al., 2009b). Our
514 results tend to support the second hypothesis, where the common ancestor to all Udoteaceae
515 species may have had a complex morphology, including the presence of a stipe, and a thallus calcified
516 and corticated throughout (*i.e.*, appendages on both the frond and stipe siphons). The simpler forms
517 may represent derived states, which appeared several times throughout the evolutionary history of
518 the family; *i.e.*, these simpler morphologies represent innovations or ecological adaptations rather
519 than reversions towards a more ancestral state.

520 This is well illustrated by the morphological character "cortication", which is often seen as a complex
521 feature but is also very relevant for the taxonomic classification of Udoteaceae. Cortication can be
522 restricted to the stipe or present throughout the thallus (*i.e.*, also on the frond). For Kooistra (2002),
523 total cortication may be ancestral because it occurs in basal lineages (*e.g.*, *Flabellia petiolata* or
524 *Udotea flabellum*) and could even predate the Udoteaceae ancestor. For this author, total thallus
525 cortication could correspond to an undifferentiated (stipe and frond similarly corticated) and
526 "primitive" state. In contrast, the presence of cortication in the stipe only may be the differentiated
527 and derived state. This hypothesis contrasts with that of other authors who consider total thallus
528 cortication to be a more evolved and complex state derived from a primitive uncorticated state
529 (Littler & Littler, 1990a). In our study, the characters related to cortication and types of secondary
530 structures (in stipe or frond) all show strong phylogenetic signals, but the total thallus cortication of
531 the ancestor appears poorly represented within the family (Fig. 3. B). Indeed, our results indicate that
532 the loss of frond cortication occurred several times independently during the evolutionary history of
533 the family and could represent convergent homoplastic evolution. This character state was
534 maintained throughout subsequent speciation events and, although more recent evolution towards

535 incomplete cortication is seen for some species (*e.g.*, in *Ventalia* gen. nov, Fig. 3. B), no reversion to
536 total cortication was observed from an uncorticated state.

537 The shape of the frond is also an important character, which has often been discussed when
538 considering the morphological complexity of Udoteaceae. Because the flabellate frond is the most
539 common character among the current Udoteaceae genera, Vroom et al. (1998) considered that the
540 hypothesis of an ancestor with a flabellate frond was more parsimonious than the hypothesis of
541 multiple independent appearances of flabellate fronds proposed by Hillis-Colinvaux (1984). Vroom et
542 al. (1998) proposed that the ancestral frond morphology may be a single flabellate frond, like those
543 of *Udotea*. This early frond may have evolved successively into three different forms: (i) the multiple
544 flabellate fronds arising from a single axis of *Rhipocephalus*, (ii) a deconstruction of the flabellate
545 frond into free siphon fronds seen in *Penicillus*, and finally in a last evolutionary jump (iii) the
546 segmented morphology of *Tydemania*. Our results indicate that the ancestral state (or plesiomorphy)
547 may have been a flabellate frond, and although it is found in most genera, this character state is
548 important for differentiating them (Fig. 3. A). The free siphons frond shape appeared several times as
549 a derived state but led to different forms simultaneously and not successively as proposed by Vroom
550 et al. (1998). In addition, while the capitulum form is homoplastic, the caespitose form or the form
551 with multiple structures (glomeruli/flabella) arising from a single axis are taxonomically informative
552 and synapomorphic for genera (Fig. 3. A). Overall, the evolution from a flabellate form to a free
553 siphon form requires further analyses before it is confirmed or refuted. In addition, these
554 evolutionary scenarios will need to be further studied to determine whether it is the result of
555 environmental adaptations (changes in environmental conditions, colonization of new ecological
556 niches), or whether it corresponds to an evolutionary advantage favored by selection.

557 The loss of character states previously considered as derived and complex (*e.g.*, presence of a stipe,
558 calcification and cortication) appear to be frequent and progressive events throughout the
559 Udoteaceae evolutionary history. Forms considered “simple”, such as *Chlorodesmis*, may be extreme

560 cases of secondary loss of complex character states. Indeed, studies have argued that the very simple
561 morphology of *Chlorodesmis* could be a case of regression to a simple primitive ancestral state or, a
562 case of neoteny for which the non-calcified "juvenile" stages may have become fertile (Meinesz,
563 1980; Kooistra, 2002). Genomic efforts combined with transcriptomics could be used to explore the
564 genes involved in morphogenesis. The observation of reproductive structures in some *Chlorodesmis*
565 species (Gepp & Gepp, 1911; Ducker, 1965, 1967) has shown that they are fertile forms and not
566 filamentous life stages of more complex and unknown species.

567 **4.2.3 Could the Udoteaceae ancestor have been calcified?** Calcification is another diagnostic
568 character for distinguishing between Udoteaceae genera. Our results show that the putative
569 Udoteaceae ancestor may have been calcified and that this character state remained as a
570 symplesiomorphy among most of the extant genera and species (Fig. 3. C). Calcification loss occurred
571 several times independently in the family's evolutionary history. It appears as a homoplastic derived
572 state (parallel evolution) in a few genera including *Chlorodesmis* s.s., *Rhipidodesmis* and *Flabellia*. This
573 result is in agreement with several published hypotheses (Kooistra, 2002; Curtis et al., 2008;
574 Verbruggen et al., 2009b). However, other studies have proposed that the Bryopsidales ancestor was
575 uncalcified. Calcification may then have been a derived state resulting from two independent
576 evolutionary events, in the suborders Halimedineae (to which Udoteaceae belongs) and
577 Bryopsidineae (*Pedobesia*) (Lam & Zechman, 2006; Verbruggen et al., 2009b). A broader phylogenetic
578 analysis and reconstruction of ancestral character states, including the Halimedineae suborder or
579 other members of the Bryopsidales, is needed to assess if calcification is a plesiomorphy (as for
580 Udoteaceae) and if the absence of calcification is an homoplastic derived state or a reversion to an
581 older ancestral state (e.g., Bryopsidales ancestor).

582 Because it makes algae less palatable and the whole thallus stronger, particularly the siphon's
583 structures, calcification was considered as an ecological advantage against herbivores (Hay et al.,
584 1994, Littler & Littler, 1990a) or when facing physical environmental pressures (Littler & Littler,

585 1990a). The occurrence of calcified and non-calcified Udoteaceae taxa was also linked to
586 environmental conditions, especially the concentration and type of environmental organic matter,
587 which is likely to influence algal metabolism through CaCO_3 precipitation (Kooistra, 2002). This could
588 explain the seasonal and alternate occurrence of calcified and non-calcified forms of *Penicillus*
589 *capitatus* in the Mediterranean (non-calcified form: *P. capitatus* f. *mediterraneus* ex- "*Espera*")
590 (Meinesz, 1980). However, the occurrence of both calcified and non-calcified taxa within the same
591 habitat (e.g., Gepp & Gepp (1911), Farghaly (1980), Littler & Littler (2000), Coppejans et al. (2001),
592 etc.) indicates that calcification does not only depend on the environment. Culture experiments are
593 needed to explore the link between calcification and environmental conditions.

594 Finally, our results highlight the correlation between calcification and the presence of a stipe (Fig. 3.
595 C, Data S5, Table S11). This corroborates observations made in some species whose calcified forms
596 have a stipe while the filamentous and non-calcified forms have none (e.g., see the work on *Penicillus*
597 by Friedman & Roth (1977) or Meinesz (1972, 1975, 1980)). The presence of a stipe is known to be
598 related to the type of anchoring substrate. Species with a stipe are most often encountered in soft
599 substrates, where calcification could help to remain erect from substrate. Soft substrates are usually
600 found in open environments exposed to grazing, where calcification could also represent a defense
601 strategy (even if the grazing pressure is lower than in the reef environment).

602 **4.2.4 Are pores and appendages functional traits?** The "window" function was introduced by Gepp
603 & Gepp (1911) for pores visible on the calcified surface of siphons or the secondary structures on
604 siphons. These two structures are believed to promote and increase contact with the surrounding
605 environment and facilitate the flow of nutrients and light inside the siphon. Like Littler & Littler
606 (1990a), we observed that species with appendages or protuberances do not have pores on the
607 surface of siphons (e.g., species of *Udotea* s.s. and *Ventalia* gen. nov.). In contrast, pores are present
608 in calcified species with naked siphons (e.g., species of *Penicillus* or *Rhipidosiphon* s.s.). Additionally,
609 our correlation tests confirmed that the presence and absence of pores and the secondary structures

610 of the frond siphons are two correlated characters (Table S11). Similarly, ancestral reconstructions
611 have shown that, in most cases, these characters are linked to evolutionary processes (pores appear
612 when appendages are lost) (Fig. 3. D and Data S5). However, some calcified species of *Ventalia* gen.
613 nov. do not have secondary structures or pores. The combination of low calcification and very thin
614 frond could explain why particular structures, such as pores and appendages which facilitate
615 exchanges with the environment, are not necessary (N.B.: Although the genus *Rhipidosiphon* s.s. is
616 monostromatic, the strong frond calcification could explain the presence of pores on the siphons
617 surface).

618 Our analysis also revealed that the presence or absence of pores and secondary structures (or
619 cortication) on the siphons were correlated (among others) to the shape and thickness of the frond
620 or to the diameter and arrangement of siphons (in one or several planes) (Table S11). This result
621 corroborates the notion of “windows” (Gepp & Gepp, 1911) and their function for the continuity of
622 exchanges between the surrounding environment and the inside of the siphon. In conclusion, the
623 presence of pores on the calcified surface of the siphons, which represents a parallel homoplastic
624 evolution (Data S5), may correspond to a functional homoplasy. In contrast, the presence of
625 appendages, which represents a symplesiomorphy (Data S5), may be a functional plesiomorphy.

626 **4.2.5 Are constriction type indicator of generic boundaries?** The type of dichotomy constrictions also
627 had a strong phylogenetic signal, and ancestral reconstruction highlighted it as an important
628 diagnostic character at the genus level (Data S5). The only exception is the genus *Chlorodesmis* s.s.,
629 which has species with various types of dichotomy constrictions. Gepp & Gepp (1991) and Littler &
630 Littler (1990a) discussed the distinct geographical patterns of this trait in *Udotea* species of the
631 Caribbean and Indo-Pacific regions. However, this pattern was less evident in our study. We found
632 that all Caribbean taxa have symmetrical constrictions, except *Udotea* s.s. species, while Indo-Pacific
633 species of *Udotea* s.s., *Glaukea* gen. nov. and *Ventalia* gen. nov have asymmetrical constrictions

634 above the dichotomies. Despite its high phylogenetic signal, the evolution and geographical
635 distribution of this character state remains difficult to explain.

636 For Farghaly (1980), this character is of no taxonomical importance because whether the
637 constrictions are “aligned” or “mismatched” (*i.e.*, symmetrical or asymmetrical, respectively)
638 accounts for the regular or irregular siphon growth rates, respectively. From our observations, we
639 believe the constrictions appear long after the branches are fully grown, and this is why apical
640 dichotomies (on the siphons margin) generally do not have constrictions yet.

641 Functionally, the constrictions help to limit the loss of cytoplasm during grazing by herbivores by
642 allowing rapid occlusion of the siphons (Duffy & Hay, 1990; Menzel et al., 1998; Vroom et al., 2001).

643 As Udoteaceae species are found in environments with different grazing pressures, the arrangement
644 of constrictions (on one or two levels) may be the result of various evolutionary adaptations to
645 specific environments.

646

647 **4.3. Systematics revisions and taxonomic treatment**

648 In this section, we discuss the revised clades (as delimited in Figure 1.B) individually, based on both
649 the molecular (species delimitation and phylogeny) and morphological (observations and
650 phylogenetic inference of character) results. We include details about the proposed systematic and
651 taxonomic revisions, species diversity, geographical distribution and diagnostic morphological
652 characters. The genera *Tydemanina* (Clade A) and *Flabellia* are not detailed here, as no taxonomic
653 changes have been applied to them (but see Lagourgue et al. (2019) for more details about the
654 morphology, diversity and distribution of *Tydemanina* species).

655

656 **4.3.1 *Udotea* sensu stricto (*Udotea* group 1- Clade B)**

657 Clade B is strongly supported (bs: 97; PP: 0.98) and contains six *Udotea* species, including the type-
658 species *U. flabellum* (J. Ellis & Sollander) M. Howe, and therefore represent *Udotea* s.s. It is
659 composed of species found in the Caribbean (*U. dixonii*, *U. dotyi*, *U. occidentalis*) and the Pacific (*U.*
660 *geppiorum*, *U. sp1*) (Figure 4). *Udotea* is strongly calcified and characterized by a stubby thallus with
661 a pluristromatic flabellate frond. The frond can be lobed and entire or divided or segmented, with
662 segments inserted in each other in a ‘tongue and groove’ arrangement (Sauvage et al., 2020). The
663 rhizoidal system is well-developed and bulbous. The frond siphons have well-developed secondary
664 structures called appendages. These latter are either dichotomously divided or lobed, and all have
665 numerous well-defined apices. The cortication is complete, *i.e.*, appendages are present throughout
666 the stipe and the frond. The specific symplesiomorphies and synapomorphies of the *Udotea* genus
667 are shown in Figure 4.

668 Considering these species as part of distinct lineage is not entirely new but had never been
669 formalized nor verified molecularly. Previous authors proposed to consider some of these species in
670 a proper group, named in turns “corticatae” (Agardh, 1887; *U. flabellum* only), an unnamed group by
671 Gepp & Gepp (1911; *U. flabellum*, *U. argentea*, *U. occidentalis*, *U. verticillosa* and *U. wilsonii*),
672 “completely corticated blade” (Nizamuddin, 1963), “*Udotea*” (Farghaly, 1980; *U. flabellum*, *U.*
673 *argentea* and *U. occidentalis*), “Flabellum” (Littler & Littler, 1990a; including only the Caribbean
674 species *U. flabellum*, *U. dixonii*, *U. dotyi*, *U. occidentalis* and *U. norrisii*), and “complete corticated
675 species” (Dragastan et al., 1997; *U. flabellum*).

676 Furthermore, Tseng & Dong (1975) described several *Udotea* species from China. Despite very brief
677 descriptions, they mention species with long and dichotomously ramified lateral branches on
678 siphons, which could refer to appendages, and could correspond to *Udotea* s.s. species (*U.*
679 *reniformis*, *U. tenax*, *U. tenuifolia*, *U. velutina* and *U. xishaensis*). Nevertheless, morphological and
680 molecular verification is needed for confirmation.

681 Species of the genus *Udotea* s.s. are characterized by limited morphological variations compared to
 682 other ex-*Udotea* species, as previously noticed by Kooistra (2002), who considered this lineage to be
 683 ancestral. Results of our time-calibrated phylogeny confirmed that *Udotea* s.s. was indeed one of the
 684 oldest genera to diverge in the family (ca 109 Ma, cf. Figure 2). This morphological resemblance
 685 between the species *in situ* could explain several erroneous identifications that have led to an
 686 overestimation of their distribution range. The genus has a wide geographical repartition, but the
 687 distribution range of species is more restricted than previously reported. For example, *U. flabellum*
 688 does not occur worldwide, but appears limited to the western tropical Atlantic (Figure 4). Similarly,
 689 we found that the Atlantic species, *U. occidentalis*, has a sister species in the Pacific, *U. sp1* (bs: 100;
 690 PP: 1), which is close morphologically (lobed aspect of the frond appendages and similar siphon
 691 diameter but different stipe appendages).

692

693 *Udotea* J. V. Lamouroux

694 **Diagnosis:** Lamouroux JVF. 1812. Sur la classification des polypiers coralligènes non entièrement
 695 pierreux. *Nouveaux Bulletin des Sciences, Société philomatiques de Paris* 3: 181–188.

696 **Type species:** *U. flabellum* (J. Ellis & Solander) M. Howe; Type: unknown; Type locality: West Indies,
 697 Basionym: *Corallina flabellum*, Ellis & Solander; Synonyms: *Udotea flabella* J.V. Lamouroux; *Udotea*
 698 *halimeda* Kützing

699 **List of species (as per this study):** *U. flabellum*, *U. occidentalis*, *U. geppiorum*, *U. dotyi*, *U. dixonii*, and
 700 *U. sp1* (new species to be described).

701 **Morphological description emended from Lamouroux (1812) and Gepp & Gepp (1911):** Flabellate,
 702 pluristromatic, corticated and highly calcified frond; Multisiphonous, corticated and calcified stipe;
 703 Continuous stipe-frond junction; Bulbous holdfast and well-developed rhizoidal system; Frond and
 704 stipe siphons with appendages, either dichotomously divided or lobed, with numerous well-defined

705 apices; Siphons dichotomously branched; Dichotomies isomorphic and not aligned; Asymmetrical
 706 supra-dichotomial constriction; Non-porous siphons sheath.

707 **Geographic distribution (confirmed using DNA sequencing): Atlantic Ocean:** Caribbean Is.

708 (Lagourgue et al., 2018; This study), Mexico (Lam and Zechman, 2006), Bermuda (Lagourgue et al.,
 709 2018), Florida (Lagourgue et al., 2018), Bahamas (Lagourgue et al., 2018), Honduras (Kooistra, 2002),
 710 Panama (Kooistra, 2002; Kooistra et al., 2002; Lagourgue et al., 2018), Jamaica (Lagourgue et al.,
 711 2018); Pacific Ocean: Hawai'i (Sauvage et al., 2016), Papua New Guinea (This study); Solomon (This
 712 study), Tonga, Fiji (Sauvage et al., 2019; This study), New Caledonia (Grande Terre, Surprises Is.,
 713 Chesterfield Is.) (This study).

714

715 **4.3.2 *Glaukea* gen. nov. (*Udotea* group 2 - Clade C)**

716 The new genus *Glaukea* (bs: 100; PP: 1, Fig. 1) is proposed to accommodate specimens previously
 717 assigned to *Udotea argenta* Zanardini (Figure 1). The genus *Glaukea* is characterized by a flabellate
 718 and zonate frond, entire or more or less divided, siphons with diameter < 80 µm and lobed
 719 appendages with rounded, swollen and convex apices (Figure 5). Our results indicate that the genus
 720 is composed of two genetically distinct species (bs: 100; PP: 1 for both; Fig. 1) that both match the
 721 very brief original diagnosis of *U. argentea* (Zanardini, 1858). However, we were unable to confirm
 722 the identity of the two species for two reasons: 1) we have no specimen from the type locality (Suez,
 723 Egypt); and 2) we could not locate the type specimen. The resolution of this case requires
 724 observations of the type specimen and the sequencing of samples from the type locality for
 725 lectotypification. This new genus is thus a complex of species that we refer to as *Glaukea argentea* 1
 726 and *G. argentea* 2 until further study provides clarification to confirm species name. In any case, this
 727 clade can no longer be considered as *Udotea* in the present assessment, considering the topology of
 728 the tree.

729 The genus *Glaukea* has retained several ancestral states and has many symplesiomorphies including
 730 a flabellate pluristromatic frond, a plurisiphonous stipe that is not ramified, with a continuous stipe-

731 frond junction, calcified siphons sheath without pores, thallus cortication, complete cortication of the
 732 frond and stipe, dichotomously ramified siphons that are arranged in one plan, and parallel to
 733 subparallel in the frond, random and isomorphic dichotomies, with asymmetrical supra-dichotomial
 734 constrictions, and appendages on frond and stipe siphons. Two synapomorphies were also
 735 highlighted including a bulbous holdfast and the presence of an erect axis. The current distribution of
 736 the genus is Indo-Pacific, with *G. argentea* 1 distributed throughout the area while *G. argentea* 2
 737 seems restricted to Madagascar.

738

739 *Glaukea* Lagourgue & Payri *gen. nov.*

740 **Type species:** *Glaukea argentea* (Zanardini) Lagourgue & Payri comb. nov.; Type: unknown; Type

741 locality: Suez, Egypt; Basionym: *Udotea argentea* Zanardini, J. 1858. Plantarum in mari Rubro

742 hucusque collectarum enumerato (juvante A. Figari). *Memoirie del Reale Istituto Veneto di Scienze,*

743 *Lettere ed Arti* 7: 209-309, pls III-XIV.

744 **List of species (as per this study):** *Glaukea argentea*, *G. sp1*. Comment: Since the type specimen is

745 unknown and no specimen of type locality could be sequenced, further studies are needed to clarify

746 the taxonomic status of the two *Glaukea* taxa.

747 **Etymology:** from the Greek "glaukos" meaning a green color with a blue tinge, in connection with the

748 color of the thallus *in situ*.

749 **Morphological description emended from Zanardini (1858) and Gepp & Gepp (1911):** Flabellate,

750 sub-reniform to lobed frond, more or less cut out, striated, zonate and pluristromatic, entire or

751 eroded upper margin, pale green-grey to ashy green; Short and not-ramified stipe, plurisiphonous,

752 with a continuous stipe-frond junction; Bulbous holdfast; The thallus is calcified with non-porous

753 siphon sheath; Siphons ramify in dichotomy and are arranged in one plan, parallel to subparallel in

754 the frond; The dichotomies are not aligned and isomorphic with asymmetrical supra-dichotomial

755 constrictions; Siphons diameter < 80 µm with decreasing size towards the apex in the blade and 25-

756 100 µm in the stipe; Total cortication of the thallus through the presence of appendages on siphons;
 757 In the frond, siphons have numerous pyriform and lobed appendages (100-200 µm long), alternately
 758 or distically arranged, constricted at the base and with rounded, swollen and convex apices; In the
 759 stipe, siphons appendages (300 -800 µm long) are dichotomously ramified (1-4 times) and digitate
 760 (“finger-like”) and with obtuse or swollen apices.

761 **Geographical distribution (confirmed using DNA sequencing):** Indian Ocean: Mayotte (This study),
 762 Scattered Islands (Glorioso Is., Juan de Nova Is.) (This study), Madagascar (This study); Pacific Ocean:
 763 Guam (Kooistra, 2002), Papua New Guinea (Cremen et al., 2019; This study). For more detailed
 764 distributions in Indo-Pacific and Red Sea, see Guiry & Guiry (2020). However, others distribution
 765 reported by solely morpho-anatomical data (Guiry & Guiry, 2020) need further verification by DNA
 766 sequencing, due to potential confusion with some *Udotea* species (e.g., *U. flabellum*, *U. geppiorum*).

768 **4.3.3 *Chlorodesmis* sensu stricto (Clade D)**

769 Based on our results, we propose to circumscribe the genus *Chlorodesmis* s.s. to the clade containing
 770 the type species *C. fastigiata* (bs: 92; PP: 0.8). This clade includes five other species, three of which
 771 are probably new (*C. sp2*, *C. sp3*, *C. sp5*), while the identification of the two others requires further
 772 verification (*C. cf. hildebrandtii* and *C. cf. major*, Figure 6). We exclude the species *C. caespitosa*,
 773 which was recovered in Clade I, and *C. baculifera*, which grouped outside of the family Udoteaceae
 774 (preliminary analyses, publication in prep). Molecular analyses of the *Chlorodesmis* species not
 775 included in our study (*C. papenfussii*, *C. dotyi*, *C. haterumana*, *C. mexicana* and *C. sinensis*) are
 776 needed to confirm their status, particularly since their morphological descriptions are relatively short
 777 (Taylor, 1945; Trono, 1971; Itono, 1973; Tseng & Dong, 1978), which makes it impossible to discuss
 778 their possible status.

779 The genus *Chlorodesmis* is characterized by an uncalcified thallus in tufts, composed of a discoid base
 780 from which arise free and interwoven siphons dichotomously divided and constricted. The
 781 symplesiomorphies and synapomorphies characterizing the genus and shown in Figure 6, are useful

782 for distinguishing the genus from other filamentous species, particularly the caespitose tufted blade,
783 the absence of cortication or the presence of supra-dichotomial constrictions. Indeed, due to their
784 relatively simple morphology, there are only few diagnostic characters available to identify
785 *Chlorodesmis* species, and this has most likely led to misidentifications in the past. Many non-
786 calcified and tufted filamentous forms belonging to other lineages and families could have been
787 confused with *Chlorodesmis* and reassessing these records, using the diagnostic characters
788 highlighted here, could reveal very different geographical distribution patterns.

789 Overall, our study confirms that the genus does not occur in the Atlantic Ocean, and its geographical
790 distribution extends throughout the Indo-Pacific. Some of the species have wide geographic
791 distribution (*e.g.*, *C. fastigiata* and *C. sp5*), while others appear more restricted (*e.g.*, *C. sp2* and *C.*
792 *sp5* in the WIO region) (Figure 6).

793

794 *Chlorodesmis* Harvey & Bailey

795 **Diagnosis:** Harvey WH, Bailey JW. 1851. Description of seventeen new species of algae, collected by
796 the United States Exploring Expedition. *Proc. Boston Soc. Nat. Sci.* 3: 370–373.

797 **Type species** = *Chlorodesmis fastigiata* (C. Agardh) S.C. Ducker; Type: LD #15661, Herb. Alg. Agardh
798 (LD); Type Locality: Mariannes Is. (Micronesia); Basionym: *Vaucheria fastigiata* C. Agardh - Synonyms:
799 *C. comosa* Harvey & Bailey; *Avrainvillea comosa* (Harvey & Bailey) G. Murray & Boodle.

800 **List of species (as per this study):** *C. fastigiata*, *C. cf. hildebrandtii*, *C. cf. major* and three new species
801 to be described (*C. sp2*, *C. sp3* and *C. sp5*).

802 **Morphological description emended from Harvey & Bailey (1851) and Gepp & Gepp (1911):**

803 Uncalcified thallus with a felted, spongy, colorless and discoid base, bearing a green tuft of free
804 and interwoven siphons; Siphons cylindrical, dichotomously branched and with numerous
805 constrictions (“pseudo-articulated” in original diagnose of Harvey & Bailey); Round or pointed apices;
806 Dichotomies iso- or anisomorphic; Symmetrical or asymmetrical supra-dichotomous constrictions
807 with ring of cell-wall for most of species.

808 **Geographical distribution (confirmed using DNA sequencing):** Indian Ocean: Mayotte (This study),
 809 Scattered Is. (Glorioso Is, Juan de Nova Is.) (This study), Madagascar (This study), Maldives Is. (This
 810 study); Pacific Ocean: Okinawa (Japan) (Sauvage et al., 2016), Guam (Verbruggen & Schils, 2012),
 811 Papua New Guinea (This study), Australia (Lizard Is.) (Kooistra, 2002), New Caledonia (Grande Terre,
 812 Surprises Is.) (This study), French Polynesia (Verbruggen et al., 2009b; This study).

813

814 **4.3.4 *Ventalia* gen. nov. (*Udotea* group 3 - Clade E)**

815 The new genus *Ventalia* is proposed to accommodate species of clade E (bs: 93; PP: 1, Fig. 7)
 816 formerly known as *Udotea orientalis*, *U. indica* and *U. papillosa*, as well as four additional taxa (*V.*
 817 *sp1*, *V. sp2*, *V. sp3* and *V. sp4*) which may represent new species (Figure 7). Each of these new species
 818 are highly supported (bs: 100; PP: 1, Fig. 7), except *Ventalia sp2*. *Ventalia* has a flabellate mono or
 819 pluristromatic frond, uncorticated (naked siphons lacking secondary structures) or pseudo-corticated
 820 siphons (*i.e.*, with rounded or spinous protuberances all around or only on the external and exposed
 821 side of the siphon) (Figure 8). The rhizoidal system is limited. The stipe is mono- or plurisiphonous,
 822 corticated or pseudo-corticated, partially or fully calcified. In plurisiphonous stipes, siphons have
 823 appendages of various aspects ranging from simple swellings to more developed structures
 824 dichotomously divided, or with terminal dichotomies only in stubby appendages (Figure 8). The
 825 siphons are thin (< 45 µm in diameter) with a porous surface and the dichotomies have asymmetrical
 826 constrictions (see Figure 7 for detailed symplesiomorphies and synapomorphies). These species are
 827 very similar morphologically and are difficult to distinguish without a thorough anatomical analysis.
 828 This is particularly true for the cryptic species without protuberances (*i.e.*, naked siphons; *V.*
 829 *orientalis*, *V. sp3* and *V. sp2*), which would not be distinguished from each other without detailed
 830 anatomical or molecular analyses.

831 A similar grouping was informally proposed by several authors: Agardh (1887) subdivided species
 832 according to the stipe cortication and included *U. orientalis* in a “Palmattae” group; Nizammudin

833 (1963) created a group for species with partially corticated frond and pointed apices; Farghaly (1980)
 834 grouped *U. indica*, *U. palmetta* and *U. papillosa* but not *U. orientalis* in a lineage called “Decaisnella”
 835 (invalid name); Finally, Gepp & Gepp (1911) considered *U. indica*, *U. palmetta*, *U. papillosa* and *U.*
 836 *orientalis* as part of a same group without naming it.

837 Although we included no sample of *U. palmetta* in our study, we believe that its morphology, as
 838 described in other studies (Decaisne, 1842; Gepp & Gepp, 1911; Farghaly, 1980) could match this
 839 new genus. Tseng & Dong (1975) also described two *Udotea* species from China (*Udotea fragifolia*
 840 and *U. renuifolia*). Despite very brief descriptions, they mention species with simple lateral branches
 841 on siphons, which could refer to protuberances, a diagnostic character of several *Ventalia* species.
 842 Morphological and molecular studies of these species are needed to confirm their transfer to
 843 *Ventalia*.

844 The geographical distribution of the genus is Indo-Pacific. The species are restricted either to the
 845 Indian Ocean (*V. papillosa*, *V. indica* but also *V. sp2* only found in Madagascar) or to the Pacific Ocean
 846 (*V. sp1* and *V. sp4*) (Figure 7). Although *U. orientalis* is recorded throughout the Indo-Pacific (Guiry &
 847 Guiry, 2020), we were only able to include Western Indian Ocean (WIO) specimens in our study.
 848 Given the possible misidentifications of the other records, further analyses of *V. orientalis* specimens
 849 from the rest of its distribution range are needed.

850

851 *Ventalia* Lagourgue & Payri **gen. nov**

852 **Type species:** *Ventalia indica* (A.Gepp & E.S.Gepp) Lagourgue & Payri **comb. nov.**

853 **List of species (as per this study):** The genus is composed of seven species: *V. orientalis*, *V. indica*, *V.*
 854 *papillosa* and four new species to be described (*V. sp1*, *V. sp2*, *V. sp3* and *V. sp4*).

855 **Etymology:** from the Greek “ventália”, with regard to the flabellate (fan-shaped) frond

856 **Morphological description:** Flabellate frond, mono or pluristromatic, uncorticated or pseudo-
 857 corticated, calcified without porous siphons sheath; Stipe mono- or plurisiphonous, corticated or

858 pseudo-corticated, partially or fully calcified; Stipe-frond junction continuous; Reduced rhizoidal
 859 system reduced; Frond siphons parallel to subparallels, naked or with protuberances; diameter <45
 860 µm; Siphon ramification by dichotomies, not aligned; Asymmetrical constrictions above dichotomies;
 861 Stipe siphons with appendages and/or ascending laterals.

862 **Geographic distribution (confirmed using DNA sequencing):** Indian Ocean: Scattered Islands (Glorioso
 863 Is., Juan de Nova Is.) (This study), Madagascar (This study); Pacific Ocean: Hawai'i (Wade & Sherwood,
 864 2017), Papua New Guinea (This study), New Caledonia (Grande Terre, Chesterfield Is., Surprises Is.)
 865 (This study).

866

867 *Ventalia indica* (A.Gepp & E.S.Gepp) Lagourgue & Payri **comb. nov.**

868 **Type:** holotype: J. A. Murray in Herb. Mus. Brit.; BM000515946

869 **Basionym:** *Udotea indica* A.Gepp & E.S. Gepp, 1911. The codiaceae of the Siboga Expedition, including
 870 a monograph of Flabellarieae and Udoteaceae. *Siboga-Expeditie* 62: 1–150.

871 **Type locality:** Karachi, Pakistan

872 **Ethymology:** pertaining to India (Latin adjective)

873 **Morphological description:** see Gepp & Gepp (1911).

874 **Geographic distribution (confirmed using DNA sequencing):** Indian Ocean: Madagascar (This study).
 875 Guiry & Guiry (2020) report an Indo-Pacific distribution, but we did not find *U. indica* specimen in the
 876 Pacific, and that should thus be genetically confirmed.

877 **List of vouchers from this study:** Madagascar, Nosy Hao, 2016: NOU203645, NOU203653.

878 **Comment:** *U. orientalis* is the most widespread species, but its type could not be located. Instead, we
 879 have chosen *U. indica* to represent the type species of *Ventalia* because its type specimen is correctly
 880 listed and deposited in BM.

881

882 Other species needing new combinations:

883 *Ventalia orientalis* (A.Gepp & E.S.Gepp) Lagourgue & Payri **comb. nov.**

884 **Basionym:** *Udotea orientalis* A.Gepp & E.S. Gepp, 1911. The codiaceae of the Siboga Expedition,
885 including a monograph of Flabellarieae and Udoteaceae. *Siboga-Expeditie* 62: 1–150.

886 **Synonym:** *Rhipidosiphon orientalis* (Gepp & Gepp) Farghaly

887 **Type:** n°s 261, 262, 263 (Siboga Expedition: Stat. 64. Island Tanah-Djampeah, 30 m.); Hildebrandt, n°
888 1918 (Lamu Harbour, Zanzibar coast, covered at low water) – Note that none of these specimens could
889 be located in a referenced Herbarium.

890 **Type locality:** syntypes localities - various in Indian and Pacific Oceans; Indonesia; Philippine Islands

891 **Ethymology:** eastern (Latin adjective)

892 **Morphological description:** see Gepp & Gepp (1911).

893 **Geographical distribution (confirmed using DNA sequencing):** Indian Ocean: Madagascar (This study).

894 *Ventalia orientalis* is recorded throughout the Indo-Pacific (Guiry & Guiry, 2020 as *Udotea orientalis*),
895 but only specimens from the Indian Ocean have been genetically verified. A molecular verification of
896 specimens recorded in the Pacific Ocean is required.

897 **List of vouchers from this study (limited to 2 per locality):** Madagascar, Nosy Mitsio, 2016:
898 NOU203674, NOU203676; Madagascar, Nosy Lava, 2016: NOU203678, NOU203680; Madagascar,
899 Radama, 2016: NOU203703, NOU203722; Madagascar, Nosy Sakatia, 2016: NOU203737; Madagascar,
900 Nosy Manitsa, 2010: PC0171887; Madagascar, Baravo Lagoon, 2010: PC0142723.

901

902 *Ventalia papillosa* (A.Gepp & E.S.Gepp) Lagourgue & Payri **comb. nov.**

903 **Basionym:** *Udotea papillosa* A. Gepp & E.S. Gepp, 1911. The codiaceae of the Siboga Expedition,
904 including a monograph of Flabellarieae and Udoteaceae. *Siboga-Expeditie* 62: 1–150.

905 **Synonym:** *Decaisnella papillosa* (Gepp & Gepp) Farghaly

906 **Type:** unknown

907 **Type locality:** syntype localities - various in Indonesia, including Noimini Bay (Teluk Noilmina), Timor.

908 **Ethymology:** papillate, covered with papillae (Latin adjective)

909 **Morphological description:** see Gepp & Gepp (1911) for the description of the species.

910 **Geographical distribution (confirmed using DNA sequencing):** Indian Ocean: Scattered Islands
 911 (Glorioso Is.) (This study), Madagascar (This study).

912 **List of vouchers from this study (limited to 2 per locality):** Madagascar, Sainte Marie Is., 2016:
 913 NOU203581, NOU203595; Madagascar, Cap Masoala, 2016: NOU203602, NOU203603; Scattered
 914 Islands, Glorioso Is., 2012: NOU087254

915

916 **4.3.5 *Rhipidosiphon* sensu stricto (Clade F)**

917 Clade F is well supported in the BI phylogeny (PP: 0.99; bs: 53) and includes the type-species *R.*
 918 *javensis*, which led us to consider the clade as representative of *Rhipidosiphon* s.s. It also includes five
 919 *Rhipidosiphon* taxa, two of which possibly correspond to new species (Figure 9). According to our
 920 species delimitation analysis (Fig.S1 & S2 SI), and morpho-anatomical data (when available), it is
 921 likely that *R.* sp2 (SSH34), *R.* sp3 (SSH 32), *R.* sp5 (SSH 55), *R.* sp 6 (SSH 56), *R.* sp8 (SSH 60) *R.* sp9 (SSH
 922 61), and *Udotea* sp10 (SSH62) belong to *Rhipidosiphon* s.s. However, missing molecular data
 923 prevented us from including them in the multilocus analysis.

924 The genus *Rhipidosiphon* s.s. is characterized by an uncorticated monostromatic flabellate frond, a
 925 stipe, which is monostromatic at the base and, in some instances, becomes plurisiphonous near the
 926 frond. The stipe is pseudo or fully uncorticated and partially calcified or fully uncalcified. A detailed
 927 list of symplesiomorphies and synapomorphies characterizing the genus *Rhipidosiphon* is shown in
 928 Figure 9. Based on our morphological and molecular results (Figures 9, S1 & S2), we propose to
 929 transfer the species *Udotea glaucescens* to this genus. This was previously suggested by Nizammudin
 930 (1963) and Farghaly (1980) but not validated (Guiry & Guiry, 2020). On the other hand, because it
 931 clustered in clade H, we propose to exclude *R. floridensis* from *Rhipidosiphon* s.s.

932 We identified the type species, *R. javensis* among our samples collected in Bunaken Island (Sulawesi,
 933 Indonesia), which is located near the type locality (Leiden Island, Nyamuk-besar, Java, Indonesia).
 934 However, the sequence of our specimen did not match with the *rbcl* sequences recorded in the

935 Genbank under the same epithet (DML40128, DML40134). Due to the strong species crypticity of the
936 genus *Rhipidosiphon*, we suspect that the specimens corresponding to the Genbank sequences could
937 have been misidentified. Besides, these specimens were collected from the Great Astrolabe Reef in
938 Fiji, which is more distant from the type locality.

939 The geographical distribution of the genus is strictly Indo-Pacific. According to Guiry & Guiry (2020),
940 the most widespread species is *R. javensis*, for which records are available throughout the Indo-
941 Pacific region. However, it is highly likely that some of these records represent erroneous
942 identifications, such as the example cited above. Therefore, it is possible that the distribution of *R.*
943 *javensis* is more restricted than previously thought, which is the case for most other species of the
944 genus (e.g., *R. glaucescens* and *R. lewmanomontiae* in the south and northwest Pacific, respectively)
945 (Figure 9).

946 However, according to the results of the individual gene trees (*tufA*, *rbcl* and 18S rDNA) (see Figures
947 S1, S2 and S4 respectively), where species do not form monophyletic clades, and due to the weak
948 root node support in the ML multilocus tree, the genus *Rhipidosiphon*, as proposed in this study,
949 remains to be confirmed. We recommend the sequencing of more species, more individuals per
950 species, as well as neighbouring clades.

951

952 *Rhipidosiphon* Littler & Littler

953 **Diagnosis:** Montagne, J.F.C. 1842. Prodromus generum specierumque phycearum novarum, in itinere
954 ad polum antarcticum...collectarum. Paris. 16 pp.

955 **Type species:** *R. javensis* Montagne; Type: PC, coll: Hombron; Type locality: Leiden Island (Nyamik-
956 besar), near Jakarta, Java, Indonesia; Synonym: *Udotea javensis* (Montagne) A. Gepp & E.S. Gepp.

957 **List of species (as per this study):** *R. javensis*, *R. lewmanomontiae*, *R. glaucescens* comb. nov. and
958 two other new species to be described (*R. sp1* and *R. sp4*).

959 **Morphological description emended from Littler & Littler (1990) and Gepp & Gepp (1911):**

960 Flabellate, calcified, monostromatic and uncorticated frond; Monosiphonous (becoming
961 plurisiphonous near the frond in some species), uncorticated or pseudo- corticated, partially or not
962 calcified; Stipe-frond junction continuous; Fine hyaline rhizoids at the base; Frond siphons cylindrical,
963 dichotomously branched, arranged in parallel to sub-parallel, without anastomosis but cemented by
964 calcification; Isomorphic dichotomies with asymmetrical constrictions above; Porous siphon sheath.

965 **Geographic distribution (confirmed using DNA sequencing):** Indian Ocean: Mayotte (This study),

966 Juan de Nova Is. (This study), Madagascar (This study), Maldive Is. (This study); Southeast-Asia:

967 Thailand (Coppejans et al., 2011), Bunaken (This study); Pacific Ocean: Okinawa (Sauvage et al.,

968 2016), Papua New Guinea (This study), Vanuatu (This study), New Caledonia (Grande Terre, Surprises
969 Is.) (This study), Fiji (Coppejans et al., 2011; This study), Tonga (This study).

970

971 New combination proposed:

972 *Rhipidosiphon glaucescens* (Harvey ex J.Agardh) Lagourgue & Payri **comb.nov.**

973 **Basionym:** *Udotea glaucescens* Harvey ex. J. Agardh (Agardh J.G. 1887. Till Algernes Systematik.Nya

974 bidrag. Acta Universitatis Lundensis 23: 1–174, 5 plates).

975 **Type locality:** Tonga

976 **Type:** Unknown

977 **Ethymology:** becoming glaucous (Latin adjective).

978 **Morphological description:** see J. Agardh (1887) and Gepp & Gepp (1911)

979 **Geographical distribution (confirmed using DNA sequencing):** Pacific Ocean: Vanuatu (This study) and

980 Fiji (This study).

981 **List of vouchers from this study:** Fiji, Nagelelevu Lagoon, 2007: NOU087262; Fiji, Heemskercq reef,

982 2007: NOU087250; Fiji, Vanua Levu, 2007: NOU087256; Vanuatu, Bridgestock point, 2006.

983

984 **4.3.6 Udoteopsis gen. nov. (Udotea group 4- Clade G)**

985 The genus *Udoteopsis* is proposed to accommodate a new species represented by specimens
986 collected in Madagascar and Mayotte (WIO region). The monospecific genus is well-supported (bs:
987 100; PP: 1, Fig. 1) but its phylogenetic relationship to the genera *Chlorodesmis*, *Ventalia* gen.nov. and
988 *Rhipidosiphon* is weakly supported (bs: 67; PP: 0.93, Fig. 1). Additional sampling is needed to confirm
989 its phylogenetic relationships within the Udoteaceae (Figure 1). The genus is characterized
990 morphologically by a monostromatic calcified flabellate frond, irregular margins with growth zones
991 where siphons are free (no calcified cement) (Figure 10). The siphons are cylindrical, naked and
992 swollen at the apices. Isolated constrictions between the dichotomies are observed and more
993 numerous in the growth area. The siphons measure 100 µm in diameter and decrease in size towards
994 the apex (50-60 µm). The dichotomies have asymmetric constrictions, and some trichotomies are
995 also observed. The stipe is multisiphonous, entirely calcified and corticated with appendages on the
996 siphons. The stipe siphons are 100 µm in diameter for a total stipe width of 500-700 µm. The calcified
997 surface of the siphons is porous to with cracks (Figure 10). The genus has several symplesiomorphies:
998 a unique flabellate frond, calcification, a plurisiphonous stipe with a continuous stipe-frond junction,
999 dichotomous siphon ramifications, primary siphons arranged in one plane, random and isomorphic
1000 dichotomies, asymmetrical constrictions, appendages on the stipe's siphons and complete stipe
1001 cortication. Synapomorphies include a monostromatic frond, a reduced rhizoidal system, an erected
1002 axis, the presence or absence of supra-dichotomial constrictions and the absence of frond
1003 cortication. The new genus is exclusively found in the WIO region and so far, only known from
1004 Mayotte and Madagascar.

1005

1006 *Udoteopsis* Lagourgue & Payri **gen. nov.**

1007 **Type species:** *Udoteopsis maiottensis* Lagourgue & Payri sp. nov.

1008 **Ethymology:** named in reference to the morphological resemblance to the genus *Udotea*.

1009 **Morphological description:** Flabellate, monostromatic and calcified frond with irregular margin;

1010 Multisiphonous, calcified and corticated stipe (500-700 µm width); Continuous stipe-frond junction;

1011 Reduced rhizoidal system; Frond siphons cylindrical and naked siphons branching dichotomously with
 1012 supra-dichotomous constrictions; Stipe siphons with appendages; Porous siphons sheath.

1013 **Geographic distribution (confirmed using DNA sequencing):** Western Indian Ocean: to date the genus
 1014 is only known from Mayotte and Madagascar (This study).

1015

1016 *Udoteopsis maiottensis* Lagourgue & Payri sp. nov.

1017 **Types:** holotype: NOU203562 (Mayotte, 2016); isotypes: NOU203560, NOU203561, NOU203570,
 1018 NOU203580 (Mayotte, 2016), NOU204161 (Mayotte, 2010), PC0171655, (Madagascar, 2010)

1019 **Type locality:** Mayotte; syntype locality: Madagascar

1020 **Ethymology:** in reference to the species type-locality, Mayotte (Latin Maiotta)

1021 **Morphological description:** Monostromatic, uncorticated, calcified, flabellate to feather-shaped
 1022 frond, irregular margin with growth and free siphons (lacking calcification cement); Multisiphonous,
 1023 corticated and calcified stipe; Stipe width of 500-700 μm ; Continuous stipe-frond junction; Reduced
 1024 rhizoidal system; Siphons cylindrical, naked and swollen at the apices in the frond, and highly
 1025 constricted in growth zone; Siphons with appendages in the stipe; Siphons branching dichotomously;
 1026 Some trichotomies; Isomorphic and not-aligned dichotomies; Asymmetrical constrictions above
 1027 dichotomies; Siphons diameter of 100 μm (in frond and stipe) decreasing toward the apex (up to 50-
 1028 60 μm) in the frond; Siphons surface porous to crack.

1029 **Geographical distribution (confirmed using DNA sequencing):** Mayotte (This study), Madagascar
 1030 (This study).

1031 **List of vouchers from this study:** Mayotte, Tanaraki, 2016: NOU203560, NOU203561, NOU203562;
 1032 Mayotte, N'gouja, 2016: NOU203570; Mayotte, Surprise Pass, 2016: NOU203580; Mayotte, 2010:
 1033 NOU204161; Madagascar, Gallions Bey, 2010: PC0171655.

1034

1035 **4.3.7 The “*Penicillus-Rhipidosiphon-Rhipocephalus-Udotea* (PRRU) complex” (Clade H)**

1036 Clade H, which is well supported (bs: 85; PP: 0.96, Fig. S5), includes specimens exclusively collected in
1037 the Western Tropical Atlantic (mostly in the Caribbean) and representing species only found in this
1038 region except for *Penicillus capitatus*, which distribution would also extend to the Mediterranean Sea
1039 (Meinesz, 1972 and 1975; see Guiry & Guiry, 2020 for more references) but this has to be confirmed
1040 genetically. Morphologically, all these species correspond to distinct and polyphyletic genera
1041 (*Udotea*, *Penicillus*, *Rhipidosiphon*, *Rhipocephalus*) (Figure S5), which results in high morphological
1042 diversity and discontinuities within this clade.

1043 Few symplesiomorphies and synapomorphies were identified for this clade. The trait inference
1044 analysis did not support the grouping of these species under a single genus. Instead, splitting the
1045 clade into three genera would appear a better option (see Fig. S5). We discuss the resulting genus
1046 hypotheses below:

1047 Genus hypothesis 1) This subclade is fully supported (bs: 100; PP: 1) and includes taxa
1048 morphologically assigned to *P. capitatus* (type species of the genus *Penicillus*), *Udotea cyathiformis*,
1049 *U. conglutinata*, *U. sp9* and the two species of *Rhipocephalus* (*R. phoenix* and *R. oblongus*). It is
1050 interesting to note that *Rhipocephalus* species used to belong to *Penicillus* until Kützing (1843a and b)
1051 described the former. Various authors also highlighted the soft morphological boundaries between
1052 the genera *Penicillus*, *Rhipocephalus* and *Udotea* (Farghaly, 1980; Kooistra, 2002). Morphologically,
1053 species in this subclade are relatively coherent and differ only by the type of siphons' arrangement
1054 (forming a coherent blade or free) and the organization of the frond (unique or composed). In light of
1055 this information, we believe that the most likely genus hypothesis for this clade is *Penicillus*.

1056 Genus hypothesis 2) The second highly supported subclade (bs: 100; PP:1, Fig. S5) of the "PRRU
1057 complex" includes species assigned to *Penicillus dumetosus*, *P. pyriformis* and *P. lamourouxii* (the
1058 latter was not included in the multilocus analysis since only one *rbcl* sequence was available, but see
1059 Figure S2). All species in this subclade are morphologically similar with a capitate (brush-shaped)
1060 frond, large siphon diameters, wide and prominent stipe appendages, with pointed (*P. dumetosus*, *P.*

1061 *pyriformis*) or finger like (*P. lamourouxii*) apices. Interestingly, Kützing (1849) already had proposed
1062 to consider these species, among others, as part of a distinct genus, *Corallocephalus*, but this latter
1063 was considered as a synonym of *Penicillus*.

1064 Genus hypothesis 3) The third subclade is represented by the species *Rhipidosiphon floridensis* only
1065 (Fig. S5 SI). However, based on the results of Lagourgue et al. (2018) and Figures S1 & S2, it is
1066 possible that *Udotea spinulosa* and *U. looensis* belong to same subclade. The situation would be
1067 similar for other *Udotea* species such as *U. luna* or *U. verticillosa*, which have never been sequenced
1068 but are morphologically close to *Udotea spinulosa* and *U. looensis*. All these species have a flabellate
1069 frond (mono or pluristromatic) composed of naked siphons or with protuberances (only on the outer
1070 face of the external siphons or at the base of the frond) and of large diameter ($\approx 50\text{-}100\ \mu\text{m}$).

1071 Additional work, particularly sequencing, is needed to confirm this clade as a genus and the species
1072 that should be included in it.

1073 Finally, the "PRRU complex" shows strong morphological discontinuities in this study, and more data
1074 are needed (specimens per species, genetic data; some species are still not genetically represented)
1075 in order to better identify the species diversity, as well as the number, composition, and phylogenetic
1076 position of the different genera included in this complex. Therefore, we choose to postpone any
1077 taxonomic decisions about the "PRRU complex" until more data is available.

1078

1079 **4.3.8 The "*Poropsis Penicillus Rhipidodesmis* complex" (PPR complex- Clade I)**

1080 This clade includes three taxa: an unknown *Poropsis* sp., *Penicillus nodulosus* and *Chlorodesmis*
1081 *caespitosa* (Figure S6).

1082 *Poropsis* sp. - Our results point out to several entities from various localities (Hawai'i, Israel, Mexico;
1083 see Figures S1 & S2), which could be considered under the name *Poropsis*, a genus previously
1084 thought to be monospecific. However, because of missing data, only one taxon was included in the

1085 multilocus analyses and is represented in Figure S6 as *Poropsis* sp. Our trait inference analysis
1086 highlighted numerous symplesiomorphies and synapomorphies, which could be useful for describing
1087 the genus. The symplesiomorphic characters include calcification, an unique tufted frond, a creeping
1088 and upright axis, a non-ramified and multisiphonous stipe, continuous stipe-frond junction,
1089 dichotomous siphon ramifications, primary siphons arranged in one plane, isomorphic dichotomies
1090 and supra-dichotomial constrictions. Synapomorphies include a reduced rhizoidal system, absence of
1091 secondary structures in frond and stipe siphons, aligned dichotomies, symmetrical constrictions and
1092 absence of frond and stipe cortication.

1093 *Penicillus nodulosus* - Following our proposed revision of the genus *Penicillus* above, *P. nodulosus*
1094 needs to be reassigned to a different genus. However, at this stage, we are missing sufficient data to
1095 make this taxonomic revision. We need genetic information about other presumed Indo-Pacific
1096 *Penicillus* species and their phylogenetic relationships among the Udoteaceae, particularly, their
1097 position within or outside this complex. Additional data is needed about the complex itself as well as
1098 the closely related species, to assess whether this species should be transferred to a particular genus
1099 or whether it should be grouped together with the other two in a same genus.

1100 *Chlorodesmis caespitosa* - Our redefinition of the genus *Chlorodesmis* s.s. above, led us to reconsider
1101 the species *Chlorodesmis caespitosa*. Interestingly, Gepp & Gepp (1911) proposed the genus
1102 *Rhipidodesmis* to accommodate the species, because it differs from other *Chlorodesmis* species by
1103 their apical branching, thicker upper filaments and the absence of moniliform and radicelliferous
1104 basal filaments. However, this was never validated taxonomically. We propose to validate the
1105 combination proposed by Gepp & Gepp (1911), including their original diagnosis, and to rename
1106 *Chlorodesmis caespitosa* (J. Agardh) as *Rhipidodesmis caespitosa* (J. Agardh) A. Gepp & E.S. Gepp.
1107 Also, our ancestral reconstructions of character states identified several symplesiomorphies and
1108 synapomorphies supporting and documenting the description of the genus *Rhipidodesmis*: the genus
1109 has a unique tufted frond, with dichotomous siphon ramifications and constrictions above the

1110 dichotomies. These three character states are symplesiomorphic. Also, the genus has several
 1111 synapomorphic character states: it is not calcified, has a discoid holdfast and an upright axis but no
 1112 stipe; The primary siphons are arranged in one plane, interwoven, with anisomorphic and aligned
 1113 dichotomies, above which the constrictions are symmetric, but do not have secondary structures,
 1114 and the frond is uncorticated.

1115

1116 *Rhipidodesmis* A. Gepp & E.S. Gepp

1117 **Diagnosis:** Gepp A, Gepp ES. 1911. The codiaceae of the Siboga Expedition, including a monograph of
 1118 Flabellarieae and Udoteaceae. Siboga-Expeditie 62: 1–150.

1119 **Type species:** *Rhipidodesmis caespitosa* (J. Agardh) Gepp & Gepp **comb. nov.**

1120 **Morphological description emended from Gepp & Gepp (1911):** Plant filamentous, gregarious, laxly
 1121 caespitose, uncalcified, composed of a discoid holdfast, and an upright axis consisting of an unique
 1122 uncorticated tufted frond but no stipe; Base decubent, colourless and irregularly ramified, very laxly
 1123 entangled (never densely felted so as to form a spurious stipes); Ascending above, viridescent,
 1124 fastigiately or flabellately ramified towards the apex; Siphons with dichotomous ramifications
 1125 (anisomorphic) and evenly (symmetrically) constricted above the dichotomies; Upper dichotomies
 1126 approximated. Siphons lacking secondary structures.

1127 **Geographical distribution (confirmed using DNA sequencing):** Pacific Ocean: New Caledonia (Grande
 1128 Terre, Surprises Is.) (This study), Papua New Guinea (This study), Hawai'i (Wade & Sherwood, 2017),
 1129 Clipperton (This study). See Guiry & Guiry (2020) for a more detailed distribution in the Indo-Pacific.

1130

1131 *Rhipidodesmis caespitosa* (J. Agardh) Gepp & Gepp

1132 **Type:** Ferguson, n° 110

1133 **Type locality:** Ceylon, Colombo, Sri Lanka

1134 **Etymology:** Latin adjective for growing in patches or tufts, caespitose (Stearn 1973)

1135 **Basionym:** *Chlorodesmis caespitosa* J.Agardh (Agardh JG. 1887. Till Algernes Systematik.Nya bidrag.
1136 Acta Universitatis Lundensis 23: 1–174, 5 plates)

1137 **Synonymes:** *Avrainvillea caespitosa* (J.Agardh) G.Murray & Boodle; *Chlorodesmis formosana* Yamada

1138 **Description:** see Gepp & Gepp (1911).

1139 **Geographical distribution (confirmed using DNA sequencing):** Pacific Ocean (confirmed with DNA
1140 sequencing): New Caledonia (Grande Terre, Surprises Is.) (This study), Papua New Guinea (This
1141 study), Hawai'i (Wade & Sherwood, 2017), Clipperton (This study). See Guiry & Guiry (2020) for a
1142 more detailed distribution in the Indo-Pacific.

1143 **List of vouchers from this study (limited to 2 per locality):** New Caledonia, Grande Terre, 2017:
1144 NOU203812; New Caledonia, Surprises Is., 2017: NOU203898; Papua New Guinea, Kavieng, 2014:
1145 NOU203345; Hawai'i, O'ahu, 2013 :HADL01229; Clipperton, 2010: NOU203464, NOU203470.

1146
1147 The phylogenetic relationships between the three taxa in this clade are strongly supported (bs: 100;
1148 PP: 1), and it would also be acceptable to group them under the same genus (Figure S6). The three
1149 taxa share several morphological characters including the shape of their moniliform siphons, with
1150 deep constrictions at the dichotomies or between them. Within this clade, *P. nodulosus* has a brush-
1151 like gross morphology, and differs from the two other taxa which are delicate and filamentous.
1152 However, *P. nodulosus* also has a filamentous form in its life cycle, as described by Harvey (1858) –
1153 moniliformous and ramified filaments arising directly from the matted-root fibres (*i.e.*, lack of stipe)
1154 –, such as the form *P. capitatus* f. *mediterraneus* (Decaisne) Huve & Huve (*i.e.*, “ex-Espera”). This
1155 filamentous form was found in our specimens of *P. nodulosus*, was confirmed genetically as
1156 belonging to the species, and could correspond to that observed by Harvey (1858). Therefore, we
1157 could hypothesize that the filamentous forms of *Poropsis* sp. and *Rhipidodesmis caespitosa* are life-
1158 stages of a more complex morphological species and considering these three taxa as part of the same
1159 genus could make sense. Conversely, numerous species hypotheses were identified in the species
1160 delimitation analyses (Fig S1 & S2) but could not be included in our multilocus phylogeny due to

1161 missing genetic data. Thus, it is likely that clade I is more diverse than currently observed in our
1162 analyses, and could be composed of several genera. Larger sampling is therefore essential to
1163 correctly delineate the species and their geographical distributions before taxonomic decisions are
1164 made for the “PPR complex”.

1165 .

1166 **CONCLUSION**

1167 Based on a total of 43 delimited species, our multilocus phylogeny revealed the monophyly of the
1168 family Udoteaceae, whereas most of its genera were polyphyletic. We propose to 1) revise the
1169 genera *Udotea* s.s., *Rhipidosiphon* s.s. and *Chlorodesmis* s.s.; 2) describe three new genera: *Glaukea*
1170 gen. nov., *Ventalia* gen. nov., and *Udoteopsis* gen. nov.; and 3) validate Gepp & Gepp's genus
1171 *Rhipidodesmis*. None of these delimited genera or their species appeared pantropical. For the first
1172 time, we produced a time-calibrated phylogeny of the family Udoteaceae. We inferred the evolution
1173 of its morpho-anatomical trait, and the taxonomic relevance of each morpho-anatomical character,
1174 for the diagnosis of the revised genera was reassessed. Numerous homoplasies were identified that
1175 remain useful for delimitating the different genera if combined with other characters. They also
1176 represent evidence of particular patterns of evolution during the diversification of Udoteaceae, such
1177 as parallel or convergent morphological evolutions or adaptations. Additionally, numerous
1178 symplesiomorphies and synapomorphies were identified and their relevance for genus-level
1179 identification was confirmed. Further study focusing on Core Halimedineae or Bryopsidales would
1180 provide information about the evolutionary patterns and taxonomic relevance of the various
1181 character states at a wider scale. Finally, considering the Udoteaceae species and genus richness, as
1182 well as their molecular and morphological diversity highlighted in this study, we believe that the
1183 taxonomic changes proposed by Cremen et al. (2019), particularly the proposal of downgrading
1184 family Udoteaceae to tribe is not justified.

1185 Acknowledgments

1186 This work was supported by the DUNE Labex-CORAIL project and ENTROPIE funds. The authors are
1187 thankful the Murray foundation and EUROMARINE for the grants that made this work possible. The
1188 authors are also grateful to Florence Rousseau, Line Le Gall, Elvan Ampou, Heroen Verbruggen and
1189 Chiela Cremen for providing additional samples or sequences. Thanks to Lydiane Mattio for
1190 proofreading the manuscript and her valuable advice. Samples were collected during several
1191 campaigns and by various collectors who we would like to acknowledge here: Bunaken, 2014 :
1192 Sample collection and DNA analyses were made possible thanks to the INDESO project, under the
1193 research permit 133/SIP/FRP/SM/V/2015 and 918/BLITBANKKP/II/2016 issued by the Indonesian
1194 government and under a material transfer agreement between BALITBANG KP (now BRSDM KP,
1195 Ministry of Maritime Affairs and Fisheries) and the IRD; Clipperton, 2010 : "Passion 2015" project
1196 financed by the «Agence française de Développement » and the Pacific Fund; Fiji, 2007: R/V Alis,
1197 BSM-Fidji, <http://dx.doi.org/10.17600/7100030>; French Polynesia, 2013 : LOF ; Kavieng, 2014:
1198 <http://dx.doi.org/10.17600/14004400>; Madagascar, 2010 : Atimo Vatae,
1199 <http://dx.doi.org/10.17600/10110040> ; 2016: R/V Antea, MAD
1200 <http://dx.doi.org/10.17600/16004700>; Madang, 2012: R/V Alis, NUIGUINI campaign
1201 <http://dx.doi.org/10.17600/12100070>; Maldive Is., 2009 : Sampling was performed with the Marine
1202 Research Center of Maldives during the 2009 Baa Atoll expedition, which did not require collection
1203 permits; Mayotte, 2010 : TARA; 2016: SIREME; New Caledonia, 2005 : R/V Alis, BSM-LOYAUTE:
1204 <http://dx.doi.org/10.17600/5100030>; 2008 : CORALCAL2 <http://dx.doi.org/10.17600/8100050>; 2012:
1205 CORALCAL4 <http://dx.doi.org/10.17600/12100060>; 2013: LOF ; 2015: R/V Alis, CHEST
1206 <http://dx.doi.org/10.17600/15004500>; 2017: R/V Alis PostBlanco1 & TARA-NC ; Scattered Islands,
1207 Glorioso Is. (2012) & Juan de Nova Is. (2013) : BIORECIE; Solomon Islands, 2004: R/V Alis, BSM-
1208 Salomon; Tonga, 2013 : PRISTINE ; Vanuatu, 2006: SANTO, <http://dx.doi.org/10.17600/6100100>.
1209

1210 **References**

- 1211
- 1212 Adamowicz SJ, Purvis A, Wills MA. 2008. Increasing morphological complexity in multiple parallel
1213 lineages of the Crustacea. *Proceedings of the National Academy of Sciences* 105: 4786–4791.
- 1214 Agardh JG. 1887. Till Algernes Systematik. Nya bidrag. *Acta Universitatis Lundensis* 23: 1–174, 5
1215 plates.
- 1216 Blomberg SP, Garland T, Ives AR. 2003. Testing for phylogenetic signal in comparative data:
1217 Behavioral traits are more labile. *Evolution* 57: 717–745.
- 1218 Bouckaert R, Heled J, Kühnert D, Vaughan T, Wu CH, Xie D, Suchard MA, Rambaut A, Drummond
1219 AJ. 2014. BEAST 2: A Software Platform for Bayesian Evolutionary Analysis (A Prlic, Ed.). *PLoS*
1220 *Computational Biology* 10: e1003537.
- 1221 Carstens BC, Knowles LL. 2007. Estimating Species Phylogeny from Gene-Tree Probabilities Despite
1222 Incomplete Lineage Sorting : An Example from *Melanoplus* Grasshoppers. *Syst. Biol* 56: 400–
1223 411.
- 1224 Carstens BC, Pelletier TA, Reid NM, Satler JD. 2013. How to fail at species delimitation. *Molecular*
1225 *Ecology* 22: 4369–4383.
- 1226 Chesters D. 2013. Collapsetypes.pl. Available at: < [https://sourceforge.net/projects/
1227 collapsetypes](https://sourceforge.net/projects/collapsetypes) >
- 1228 Collado-Vides L, Suárez A, Cabrera R. 2009. Una revisión taxonómica del género *Udotea* en el
1229 Caribe mexicano y cubano. *Rev. Invest. Mar* 30: 145–161.
- 1230 Coppejans E, Leliaert F, Dargent O, De Clerck O. 2001. Marine green algae (Chlorophyta) from the
1231 north coast of Papua New Guinea. *Cryptogamie, Algol.*, 22: 375–443.
- 1232 Coppejans E, Leliaert F, Verbruggen H, Prathep A, De Clerck O. 2011. *Rhipidosiphon*
1233 *lewmanomontiae* sp. nov. (Bryopsidales, Chlorophyta), a calcified udoteacean alga from the
1234 central Indo-Pacific based on morphological and molecular investigations. *Phycologia* 50: 403–
1235 412.

- 1236 Cremen MCM, Leliaert F, West J, Lam DW, Shimada S, Lopez-Bautista JM, Verbruggen H. 2019.
1237 Reassessment of the classification of Bryopsidales (Chlorophyta) based on chloroplast
1238 phylogenomic analyses. *Molecular Phylogenetics and Evolution* 130: 397–405.
- 1239 Curtis NE, Dawes CJ, Pierce SK. 2008. Phylogenetic analysis of the large subunit rubisco gene
1240 supports the exclusion of *Avrainvillea* and *Cladocephalus* from the Udoteaceae (Bryopsidales,
1241 Chlorophyta). *Journal of Phycology* 44: 761–767.
- 1242 Dayrat B. 2005. Towards integrative taxonomy. *Biol. J. Linn. Soc. Lond.* 85: 407–415.
- 1243 Decaisne J. 1842. Mémoire sur les corallines ou polypiers calcifères. *Annales des Sciences*
1244 *Naturelles, Botanique, Seconde Série* 18: 96–128.
- 1245 Dragastan O, Richter DK, Kube B, Popa M, Sarbu A, Ciugulea I. 1997. A new family of paleo-
1246 mesozoic calcareous green siphons-algae (Order Bryopsidales, Class Bryosidophyceae, Phylum
1247 Siphonophyta). *Rev. Espanola de Micropaleontologia* 29: 69–135.
- 1248 Drummond AJ, Ho SYW, Phillips MJ, Rambaut A. 2006. Relaxed Phylogenetics and Dating with
1249 Confidence (D Penny, Ed.). *PLoS Biology* 4: 699–710.
- 1250 Drummond AJ, Xie W, Heled J. 2012. Bayesian Inference of Species Trees from Multilocus Data
1251 using * BEAST. : 1–18.
- 1252 Dubois A. 2007. Naming taxa from cladograms: A cautionary tale. *Molecular Phylogenetics and*
1253 *Evolution* 42: 317–330.
- 1254 Ducker SC. 1965. The Structure and Reproduction of the Green Alga *Chlorodesmis bulbosa*.
1255 *Phycologia* 4: 149–162.
- 1256 Ducker S. 1967. The genus *Chlorodesmis* (Chlorophyta) in the Indo-Pacific region. *Nova Hedwigia*
1257 13: 145–182.
- 1258 Dupuis JuR, Roe AD, Sperling FAH. 2012. Multi-locus species delimitation in closely related animals
1259 and fungi: one marker is not enough. *Molecular Ecology* 21: 4422–4436.
- 1260 Egerod LE. 1952. An analysis of the siphonous Chlorophycophyta with special reference to the
1261 Siphonocladales, Siphonales, and Dasycladales of Hawaii. *Univ. Calif. Publ. Bot* 25: 327–367.

- 1262 Farghaly M. 1980. Algues Benthiques de la Mer Rouge et du bassin occidental de l'océan Indien.
1263 Unpublished thesis, Université des sciences et techniques du Languedoc.
- 1264 Fiore M. 1936. Di un'alga fossile nuova per la "Pesciara" di Bolca, Nota.
- 1265 Friedmann EI, Roth WC. 1977. Development of the siphonous green alga *Penicillus* and the *Espera*
1266 state. *Botanical Journal of the Linnean Society* 74: 189–214.
- 1267 Fritz SA, Purvis A. 2010. Selectivity in mammalian extinction risk and threat types: A new measure
1268 of phylogenetic signal strength in binary traits. *Conservation Biology* 24: 1042–1051.
- 1269 Fujita MK, Leache AD, Burbrink FT, Mcguire JA, Moritz C. 2012. Coalescent-based species
1270 delimitation in an integrative taxonomy. *Trends Ecol. Evol.* 27: 480–488.
- 1271 Garbino GST, Martins-Junior AMG. 2018. Phenotypic evolution in marmoset and tamarin monkeys
1272 (Cebidae, Callitrichinae) and a revised genus-level classification. *Molecular Phylogenetics and*
1273 *Evolution* 118: 156–171.
- 1274 Gepp A, Gepp ES. 1911. The codiaceae of the Siboga Expedition, including a monograph of
1275 Flabellarieae and Udoteaceae. *Siboga-Expeditie* 62: 1–150.
- 1276 Goreau TF. 1963. Calcium carbonate deposition by coralline algae and corals in relation to their
1277 roles as reef-builders. *Annals of the New York Academy of Sciences* 109:127-67.
- 1278 Granier B. 2012. The contribution of calcareous green algae to the production of limestones: a
1279 review. *Geodiversitas* 34, 35–60. doi:10.5252/g2012n1a3
- 1280 Guiry MD, Guiry GM. 2020. AlgaeBase. World-wide electronic publication, National University of
1281 Ireland, Galway. <http://www.algaebase.org>; searched on 13 January 2020
- 1282 Gustavson TC, Delevoryas T. 1992. *Caulerpa*-like marine alga from Permian strata, Palo Duro Basin,
1283 West Texas. *Journal of Paleontology* 66: 160–161.
- 1284 Händeler K, Wägele H, Wahrmund U, Rüdinger M, Knoop V. 2010. Slugs' last meals: molecular
1285 identification of sequestered chloroplasts from different algal origins in Sacoglossa
1286 (Opisthobranchia, Gastropoda). *Molecular Ecology Resources* 10: 968–978.
- 1287 Harmon LJ, Weir JT, Brock CD, Glor RE, Challenger W. 2008. GEIGER: Investigating evolutionary

- 1288 radiations. *Bioinformatics* 24: 129–131.
- 1289 Harvey WH, Bailey JW. 1851. Description of seventeen new species of algae, collected by the
1290 United States Exploring Expedition. *Proc. Boston Soc. Nat. Sci.* 3: 370–373.
- 1291 Hay ME, Kappel QE, Fenical W. 1994. Synergisms in Plant Defenses against Herbivores: Interactions
1292 of Chemistry, Calcification, and Plant Quality. *Ecology* 75: 1714–1726.
- 1293 Heled J, Drummond AJ. 2012. Calibrated Tree Priors for Relaxed Phylogenetics and Divergence
1294 Time Estimation. *Systematic Biology* 61: 138–149.
- 1295 Hillis-Colinvaux L. 1984. Systematics of the Siphonales. Irvine, D. E. G. & John, D. M. [Eds.]
1296 *Systematics of the Green Algae*. London and Orlando, Florida, 271–296.
- 1297 Itono I. 1973. Notes on Marine Algae from Hateruma Island, Ryukyu. *Botanical Magazine, Tokyo*
1298 86: 155–168.
- 1299 Kapli P, Lutteropp S, Zhang J, Kobert K, Pavlidis P, Stamatakis A, Flouri T. 2017. Multi-rate Poisson
1300 Tree Processes for single-locus species delimitation under Maximum Likelihood and Markov
1301 Chain Monte Carlo. *Bioinformatics* 29: btx025.
- 1302 Kearse M, Moir R, Wilson A, Stones-Havas S, Cheung M, Sturrock S, Buxton S, Cooper A, Markowitz
1303 S, Duran C, Thierer T, Ashton B, Meintjes P, Drummond A. 2012. Geneious Basic: An integrated
1304 and extendable desktop software platform for the organization and analysis of sequence data.
1305 *Bioinformatics* 28: 1647–1649.
- 1306 Kooistra WHCF. 2002. Molecular phylogenies of Udoteaceae (Bryopsidales, Chlorophyta) reveal
1307 nonmonophyly for *Udotea*, *Penicillus* and *Chlorodesmis*. *Phycologia* 41: 453–462.
- 1308 Kooistra WCF, Coppejans EGG, Payri C. 2002. Molecular systematics, historical ecology, and
1309 phylogeography of *Halimeda* (Bryopsidales). *Molecular Phylogenetics and Evolution* 24: 121–
1310 138.
- 1311 Kützing FT. 1843a. *Phycologia generalis oder Anatomie, Physiologie und Systemkunde der Tange*
1312 (F. A. Brockhaus, Ed.). Leipzig: Brockhaus, F. A.
- 1313 Kützing FT. 1843b. Ueber die Systematische Eintheilung der Algen. *Linnaea* 17: 75–107.

- 1314 Kützing FT. 1849. *Species Algarum* (FA Brockhaus, Ed.). Lipsiae [Leipzig]: Brockhaus, F. A.
- 1315 Lagourgue L, Puillandre N, Payri CE. 2018. Exploring the Udoteaceae diversity (Bryopsidales,
1316 Chlorophyta) in the Caribbean region based on molecular and morphological data. *Molecular*
1317 *Phylogenetics and Evolution* 127: 758–769.
- 1318 Lam DW, Zechman FW. 2006. Phylogenetic analyses of the Bryopsidales (Ulvophyceae,
1319 Chlorophyta) based on Rubisco large subunit gene sequences. *Journal of Phycology* 42: 669–
1320 678.
- 1321 Lamouroux JVF. 1812. Sur la classification des polypiers coralligènes non entièrement pierreux.
1322 *Nouveaux Bulletin des Sciences, Societé philomatiques de Paris* 3: 181–188.
- 1323 Lanfear R, Calcott B, Ho SYW, Guindon S. 2012. PartitionFinder: Combined Selection of Partitioning
1324 Schemes and Substitution Models for Phylogenetic Analyses. *Molecular Biology and Evolution*
1325 29: 1695–1701.
- 1326 Leliaert F, Verbruggen H, Vanormelingen P, Steen F, López-Bautista JM, Zuccarello GC, De Clerck
1327 O. 2014. DNA-based species delimitation in algae. *European Journal of Phycology*.
- 1328 Littler DS, Littler MM. 1990a. Systematics of *Udotea* species (Bryopsidales, Chlorophyta) in the
1329 tropical western Atlantic. *Phycologia* 29: 206–252.
- 1330 Littler DS, Littler MM. 1990b. Reestablishment of the green algal genus *Rhipidosiphon* Montagne
1331 (Udoteaceae, Bryopsidales) with a description of *Rhipidosiphon floridensis* sp. nov. *British*
1332 *Phycological Journal* 25: 33–38.
- 1333 Littler MM, Littler DS. 1999. Blade abandonment/proliferation: A novel mechanism for rapid
1334 epiphyte control in marine macrophytes. *Ecology* 80: 1736–1746.
- 1335 Littler DS, Littler MM. 2000. *Caribbean Reef Plants: An Identification Guide to the Reef Plants of the*
1336 *Caribbean, Bahamas, Florida and Gulf of Mexico* (I Offshore Graphics, Ed.). Washington, D.C.
- 1337 Meinesz A. 1972. Sur la croissance et le développement du *Penicillus capitatus* Lamarck forma
1338 mediterranea (Decaisne) P. et H. Huv, (Caulerpale, Udot,ac,e). *Comptes Rendus de l'Académie*
1339 *des Sciences Paris* 275: 667–669.

- 1340 Meinesz A. 1975. Premières observations sur la reproduction du *Penicillus capitatus* Lamarck
1341 forma *mediterranea* (Decaisne) P. et H. Huve (Caulerpale, Udoteaceae). *Annales du Museum*
1342 *d'Histoire Naturelle de Nice* 3: 19–20.
- 1343 Meinesz A. 1980. Connaissances actuelles et contribution à l'étude de la reproduction et du cycle
1344 des Udotéacées (Caulerpales, Chlorophytes). *Phycologia* 19: 110–138.
- 1345 Miller MA, Pfeiffer W, Schwartz T. 2010. Creating the CIPRES Science Gateway for inference of
1346 large phylogenetic trees. *2010 Gateway Computing Environments Workshop (GCE)*. IEEE, 1–8.
- 1347 Monaghan MT, Wild R, Elliot M, Fujisawa T, Balke M, Inward DJG, Lees DC, Ranaivosolo R, Eggleton
1348 P, Barraclough TG, Vogler AP. 2009. Accelerated species Inventory on Madagascar using
1349 coalescent-based models of species Delineation. *Systematic Biology* 58: 298–311.
- 1350 Montagne JFC. 1842. Prodrômus generum specierumque phycearum novarum, in itinere ad polum
1351 antarcticum...collectarum. Paris. 16 pp.
- 1352 Nizamuddin M. 1963. Studies on the Green Alga, *Udotea indica* A. & E. S. Gepp, 1911. *Pacific*
1353 *Science* 17: 243–245.
- 1354 Orme D. 2013. The caper package: comparative analysis of phylogenetics and evolution in R.
- 1355 Pagel M. 1999. Inferring the historical patterns of biological evolution. *Nature* 401: 877–884.
- 1356 Payri CE. 2000. Production primaire et calcification des algues benthiques en milieu corallien.
1357 *Océanis* 26, 427–463
- 1358 Payri CE, Verbruggen H. 2009. *Pseudocodium mucronatum*, a new species from new caledonia, and
1359 an analysis of the evolution of climatic preferences in the genus (Bryopsidales, Chlorophyta).
1360 *Journal of Phycology* 45: 953–961.
- 1361 Pigliucci M. 2008. Is evolvability evolvable? *Nature Reviews Genetics* 9: 75–82.
- 1362 Poncet J. 1989. Presence du genre *Halimeda* Lamouroux, 1812 (algue verte calcaire) dans le
1363 Permien Supérieur du Sud Tunisien. *Revue Micropaleontologie* 32: 40–44.
- 1364 Pons J, Barraclough TG, Gomez-zurita J, Cardoso A, Duran DP, Hazell S, Kamoun S, Sumlin WD,
1365 Vogler AP. 2006. Sequence-Based Species Delimitation for the DNA Taxonomy of Undescribed

- 1366 Insects. *Syst. Biol* 55: 595–609.
- 1367 Puillandre N, Lambert A, Brouillet S, Achaz G. 2012a. ABGD , Automatic Barcode Gap Discovery for
1368 primary species delimitation. *Molecular Biology and Evolution*: 1864–1877.
- 1369 Puillandre N, Modica MV, Gustave O, Place LL, West CP. 2012b. Large-scale species delimitation
1370 method for hyperdiverse groups. *Molecular Ecology*: 1–21.
- 1371 R Development Core Team. 2019. R: A language and Environment for Statistical Computing.
- 1372 Rabosky DL, Santini F, Eastman J, Smith SA, Sidlauskas B, Chang J, Alfaro ME. 2013. Rates of
1373 speciation and morphological evolution are correlated across the largest vertebrate radiation.
1374 *Nature Communications* 4: 1–8.
- 1375 Rambaut A, Drummond A. 2007. Tracer version 1.5.
- 1376 Rannala B. 2015. The art and science of species delimitation. *Current Zoology*.
- 1377 Reid NM, Carstens BC. 2012. Phylogenetic estimation error can decrease the accuracy of species
1378 delimitation : a Bayesian implementation of the general mixed Yule-coalescent model. *BMC*
1379 *Evolutionary Biology*: 1–11.
- 1380 Revell LJ. 2012. phytools: an R package for phylogenetic comparative biology (and other things).
1381 *Methods in Ecology and Evolution* 3: 217–223.
- 1382 Ries J.B. 2006. Aragonitic algae in calcite seas: effect of seawater mg/ca ratio on algal sediment
1383 production. *Journal of Sedimentary Research*. 76, 515–523. doi:10.2110/jsr.2006.051
- 1384 Ronquist F, Huelsenbeck JP. 2003. MrBayes 3: Bayesian phylogenetic inference under mixed
1385 models. *Bioinformatics (Oxford, England)* 19: 1572–4.
- 1386 Saunders GW, Kucera H. 2010. An evaluation of rbcL, tufA, UPA, LSU and ITS as DNA barcode
1387 markers for the marine green macroalgae. *Cryptogamie Algologie*: 487–528.
- 1388 Sauvage T, Ballantine DL, Peyton KA, Wade RM, Sherwood AR, Keeley S, Smith C. 2019. Molecular
1389 confirmation and morphological reassessment of *Udotea geppiorum* (Bryopsidales,
1390 Chlorophyta) with ecological observations of mesophotic meadows in the Main Hawaiian
1391 Islands. *European Journal of Phycology* 00: 1–11.

- 1392 Sauvage T, Payri CE, Draisma SG, Prud WF, Van Reine H, Verbruggen H, Belton GS, Frederico Gurgel
1393 CD, Gabriel D, Sherwood AR, Fredericq S, Sga D, Van Reine HW, Cfd G. 2013. Molecular diversity
1394 of the *Caulerpa racemosa-Caulerpa peltata* complex (Caulerpaceae, Bryopsidales) in New
1395 Caledonia, with new Australasian records for *C. racemosa* var. *cylindracea*. *Phycologia* 52: 6–
1396 13.
- 1397 Sauvage T, Schmidt WE, Suda S, Fredericq S. 2016. A metabarcoding framework for facilitated
1398 survey of endolithic phototrophs with tufA. *BMC Ecology* 16: 1–21.
- 1399 Schlick-Steiner BC, Steiner FM, Seifert B, Stauffer C, Christian E, Crozier RH. 2010. Integrative
1400 Taxonomy: A Multisource Approach to Exploring Biodiversity. *Annual Review of Entomology*
1401 55: 421–438.
- 1402 Stamatakis A. 2014. RAxML version 8: a tool for phylogenetic analysis and post-analysis of large
1403 phylogenies. *Bioinformatics* 30: 1312–1313.
- 1404 Stamatakis A, Hoover P, Rougemont J, Renner S. 2008. A Rapid Bootstrap Algorithm for the RAxML
1405 Web Servers. *Systematic Biology* 57: 758–771.
- 1406 Talavera G, Dinc V, Vila R. 2013. Factors affecting species delimitations with the GMYC model :
1407 insights from a butterfly survey. 1101–1110.
- 1408 Tamura K, Stecher G, Peterson D, Filipski A, Kumar S. 2013. MEGA6: Molecular Evolutionary
1409 Genetics Analysis version 6.0. *Molecular biology and evolution* 30: 2725–9.
- 1410 Taylor WR. 1945. Pacific marine algae of the Allan Hancock Expedition to the Galapagos Islands.
1411 *Allan Hancock Pacific Expeditions* 12: 1–518.
- 1412 Thiers B. 2018. Index Herbariorum: A Global Directory of Public Herbaria and Associated Staff. New
1413 York Botanical Garden's Virtual Herbarium.
- 1414 Trono GC. 1971. Some new species of marine benthic algae from the Caroline Islands, western-
1415 central Pacific. *Micronesica* 7: 45–77.
- 1416 Tseng CK, Dong ML. 1975. Some new species of *Udotea* from the Xisha Islands, Guangdong
1417 Province, China. *Studia Marina Sinica* 10: 1–19, pls I, II.

- 1418 Tseng CK, Dong ML. 1978. Studies on some marine green algae from the Xisha Islands, Guangdong
1419 Province, China. I. *Studia Marina Sinica* 12: 41–50.
- 1420 Verbruggen H, Ashworth M, LoDuca ST, Vlaeminck C, Cocquyt E, Sauvage T, Zechman FW, Littler
1421 DS, Littler MM, Leliaert F, De Clerck O. 2009b. A multi-locus time-calibrated phylogeny of the
1422 siphonous green algae. *Molecular Phylogenetics and Evolution* 50: 642–653.
- 1423 Verbruggen H, De Clerck O, Cocquyt E, Kooistra WHCF, Coppejans E. 2005a. Morphometric
1424 taxonomy of siphonous green algae: a methodological study within the genus *Halimeda*
1425 (Bryopsidales). *J. Phycological* 41: 126–139.
- 1426 Verbruggen H, De Clerck O, Kooistra, Wiebe HCF, Coppejans E. 2005b. Molecular and
1427 morphometric data pinpoint species boundaries in *Halimeda* section *Rhipsalis* (Bryopsidales,
1428 Chlorophyta) . *J. Phycological* 41: 606–621.
- 1429 Verbruggen H, Leliaert F, Maggs CA, Shimada S, Schils T, Provan J, Booth D, Murphy S, De Clerck O,
1430 Littler DS, Littler MM, Coppejans E. 2007. Species boundaries and phylogenetic relationships
1431 within the green algal genus *Codium* (Bryopsidales) based on plastid DNA sequences.
1432 *Molecular Phylogenetics and Evolution* 44: 240–254.
- 1433 Verbruggen H, Marcelino VR, Guiry MD, Cremen MCM, Jackson CJ. 2017. Phylogenetic position of
1434 the coral symbiont *Ostreobium* (Ulvophyceae) inferred from chloroplast genome data (L
1435 Graham, Ed.). *Journal of Phycology* 53: 790–803.
- 1436 Verbruggen H, Schils T. 2012. *Rhipilia coppejansii*, a new coral reef-associated species from Guam
1437 (Bryopsidales, Chlorophyta). *Journal of Phycology* 48: 1090–1098.
- 1438 Verbruggen H, Tyberghein L, Pauly K, Vlaeminck C, Nieuwenhuyze K Van, Kooistra WHCF, Leliaert
1439 F, Clerck O De. 2009c. Macroecology meets macroevolution: evolutionary niche dynamics in
1440 the seaweed *Halimeda*. *Global Ecology and Biogeography* 18: 393–405.
- 1441 Verbruggen H, Vlaeminck C, Sauvage T, Sherwood AR, Leliaert F, De Clerck O. 2009a. Phylogenetic
1442 analysis of pseudochlorodesmis strains reveals cryptic diversity above the family level in the
1443 siphonous green algae (bryopsidales, chlorophyta). *Journal of Phycology* 45: 726–731.

- 1444 Vroom PS, Smith CM, Keeley SC. 1998. Cladistics of the Bryopsidales: A preliminary analysis. 360:
1445 351–360.
- 1446 Wade RM, Sherwood AR. 2017. Molecular determination of kleptoplast origins from the sea slug
1447 *Plakobranthus ocellatus* (Sacoglossa, Gastropoda) reveals cryptic bryopsidalean (Chlorophyta)
1448 diversity in the Hawaiian Islands. *Journal of Phycology* 53: 467–475.
- 1449 Wiens JJ. 2007. Species delimitation: new approaches for discovering diversity. *Systematic biology*
1450 56: 875–878.
- 1451 Wray, J. L. 1977. *Calcareous Algae*. Elsevier, Amsterdam, 185 pp
- 1452 Zanardini G. 1858. *Plantarum in mari Rubro hucusque collectarum enumerato* (juvante A. Figari).
1453 *Memoirie del Reale Istituto Veneto di Scienze, Lettere ed Arti* 7: 209–309, pls III-XIV.
- 1454 Zhang J, Kapli P, Pavlidis P, Stamatakis A. 2013. A general species delimitation method with
1455 applications to phylogenetic placements. *Bioinformatics* 29: 2869–2876.
- 1456

1457 **Tables**

1458 **Table 1:** Number of delimited PSHs, for each of the five methods applied to *tufA* and *rbcl*, including
 1459 the number of singletons.

1460

Methods		GMYC	bGMYC	hPTP	mPTP	ABGD
Number of delimited PSHs number of singletons	<i>tufA</i>	39 5	43 8	53 17	50 14	51 10
	<i>rbcl</i>	49 13	48 13	56 27	53 20	55 17

1461

1462 **Table 2:** Main results of the trait evolution mapping for the discrete morpho-anatomical characters having a phylogenetical signal and for which the
 1463 ancestral state could be estimated for the Udoteaceae ancestor. Status of each character state (homoplasy, synapomorphy or symplesiomorphy) is also
 1464 reported.

1465

CHARACTERS	STATUS AND TAXONOMIC RELEVANCE	STATE ESTIMATION FOR THE UDOTEACEAE ANCESTOR
Stipe (presence/absence)	Presence: symplesiomorphy; Absence: homoplasy/synapomorphy	Presence of stipe
Calcification (presence/absence)	Presence: symplesiomorphy; Absence: homoplasy/synapomorphy	Calcified
Calcified siphons surface porous or non-porous	Non-porous: symplesiomorphy; Porous: homoplasy	Non porous
Stipe type	Multisiphonous: symplesiomorphy; Monosiphonous: homoplasy	Multisiphonous
Primary siphons disposition	On one plane: symplesiomorphy; On several planes: homoplasy/synapomorphy	On one plane
External habit (Growth)	Creeping and upright axis: symplesiomorphy; Only upright axis: synapomorphy	Creeping and upright
Thallus cortication	Total cortication: symplesiomorphy; Partial cortication: homoplasy; Absence of cortication: homoplasy/synapomorphy	Total cortication of the thallus
Fronnd shape	Flabellate: symplesiomorphy; Capitata: homoplasy; Caespitose: homoplasy/synapomorphy; Axis with different structures: synapomorphy; Cyathiform and filiform: autapomorphies	Flabellate
Fronnd thickness	Pluristromatic (or in tuft): symplesiomorphy; Monostromatic: homoplasy/synapomorphy	Pluristromatic
Secondary structures on the frond siphon	Appendages: symplesiomorphy; Protuberances: homoplasy; None: homoplasy/synapomorphy	Appendages
Fronnd cortication	Complete cortication: symplesiomorphy; Incomplete cortication: homoplasy; Absence of cortication: homoplasy/synapomorphy	Complete cortication of the frond
Dichotomies alignment	Not aligned: symplesiomorphy; Aligned: homoplasy; Aligned only at the basis: homoplasy/synapomorphy	Not aligned
Type of constrictions	Asymmetrical: symplesiomorphy; Symmetrical: homoplasy/synapomorphy	Asymmetrical
Secondary structures on the stipe siphon	Appendages: symplesiomorphy; Descending laterals: homoplasy; None: homoplasy/synapomorphy	Appendages
Stipe cortication	Complete cortication: symplesiomorphy; Pseudocortex: homoplasy; Absence of cortication: homoplasy/synapomorphy	Complete cortication of the stipe
Stipe-fronnd junction	Continuous: symplesiomorphy; Sharp: homoplasy	Continuous

1466

1467

1468 **Figures Legends**

1469 **Figure 1. A**, ML phylogeny produced using the multi-marker matrix (*tufA*, *rbcL* and 18S rDNA) with
 1470 bootstraps and posterior probabilities indicated at nodes (bs/PP). Species of the same genus as
 1471 recognized by Guiry & Guiry (2020, searched on January 2020) are indicated using the same color. (*)
 1472 indicates type species. **B**, Condensed ML tree showing the nine clades (A-I) proposed for the
 1473 taxonomic revision of Udoteaceae genera. Clades A, B, D and F represent current genera whose
 1474 taxonomic boundaries are redefined in this study. Clades C, E, and G represent new genera, while the
 1475 status of clades H and I remains unclear.

1476 **Figure 2.** Time-calibrated phylogeny of the Udoteaceae from the BEAST analysis. Estimated
 1477 divergence times are indicated at the nodes, and grey bars indicate the 95% HPD (highest probability
 1478 densities). Black asterisks represent nodes supported for both the ML and Bayesian Inference
 1479 methods ($bs > 85$; $PP > 0.95$), while grey asterisks represent nodes that are only supported in the BI
 1480 analysis ($PP > 0.95$; $bs < 85$). Asterisks after taxon names indicate invalid genus or species requiring
 1481 taxonomic revision.

1482 Figure 3: Ancestral state reconstruction for **A**, Upright vegetative form; **B**, Thallus cortication; **C**,
 1483 Presence or absence of calcification; and **D**, Presence or absence of secondary structures on frond
 1484 siphons. The analyses were carried out using MCCT resulting from the BEAST analysis and 1,000
 1485 iterations. Pie charts show the frequency of character states at each node.

1486 **Figure 4.** ML phylogeny of *Udotea* s.s. Bootstraps and Posterior probabilities (bs/PP) are indicated at
 1487 nodes. Species hypotheses obtained using the five species delimitation methods on the two markers
 1488 are shown on the right, along with allocated species names, illustrations and geographical
 1489 distribution (A= *U. flabellum*; B= *U. dotyi*; C= *U. dixonii*; D= *U. occidentalis*; E= *U. geppiorum*; F= *U.*
 1490 sp1). The genus symplesiomorphies and synapomorphies, which were identified by inferring
 1491 morphological characters on the time-calibrated phylogeny, are shown on the left. Image rights:
 1492 Payri, C.E.; Menou, J.L., Littler & Littler (2000;*).

1493 **Figure 5.** *Glaukea* genus. **A-D**, *Glaukea argentea* 1 (NOU204097; NOU204098). **A**, Herbarium
 1494 specimen. **B**, *In situ* specimen. **C**, Siphons with lobed appendages. **D**, Lobed appendages. **E-H**, *G.*
 1495 *argentea* 2 (NOU203657, NOU203661). **E**, Herbarium specimen. **F**, *In situ* specimen. **G**, Siphons with
 1496 lobed appendages. **H**, Lobed appendages; Scale bars: B= 4 cm; C= 80 μ m; D= 57 μ m; F= 2.3 cm; G=
 1497 120 μ m; H= 37.5 μ m.

1498 **Figure 6.** ML phylogeny of *Chlorodesmis*. Bootstraps and Posterior probabilities (bs/PP) are indicated
 1499 at nodes. Species hypotheses obtained using the five species delimitation methods on the two
 1500 markers are shown on the right, along with allocated species names, illustrations and geographical
 1501 distribution (B= *C. cf. hildebrandtii*; C= *C. cf. major*; D= *C. sp3*; F= *C. sp2*). The genus
 1502 symplesiomorphies and synapomorphies, which were identified by inferring morphological
 1503 characters on the time-calibrated phylogeny, are shown on the left. Abbreviations: PNG, Papua New
 1504 Guinea. Image rights: Payri, C.E

1505 **Figure 7.** ML phylogeny of *Ventalia* gen.nov. Bootstraps and Posterior probabilities (bs/PP) are
 1506 indicated at nodes. Species hypotheses obtained using the five species delimitation methods on the
 1507 two markers are presented on the right, along with allocated species names, illustrations and
 1508 geographical distribution (A= *V. sp1*; D= *V. orientalis*; E = *V. sp2.*; H= *V. sp4*). The genus
 1509 symplesiomorphies and the synapomorphy, which were identified by inferring morphological
 1510 characters on the time-calibrated phylogeny, are indicated on the left. Image rights: Payri, C.E.;
 1511 Lasne, G.

1512 **Figure 8.** *Ventalia* genus. **A-D**, *Ventalia indica* (NOU203645-8). **A**, Herbarium specimen. **B**, *In situ*
 1513 specimen. **C**, Blade siphons with protuberances. **D**, Stipe siphon with dichotomously divided
 1514 appendages. **E-H**, *Ventalia orientalis* (NOU203718-722; NOU203680; NOU203683). **E**, Herbarium
 1515 specimen. **F**, *In situ* specimen. **G**, Smooth blade siphon. **H**, Stipe siphon with dichotomously divided
 1516 appendages. **I-L**, *Ventalia papillosa* (NOU203603; NOU203587). **I**, Herbarium specimen. **J**, *In situ*
 1517 specimen. **K**, Blade siphons with protuberances. **L**, Stipe siphon with dichotomously divided

1518 appendages. Scale bars: B= 3 cm; C= 80 μ m; D= 65 μ m; F= 0.8 cm; G= 80 μ m; H= 65 μ m; J= 0.7 cm; K=
 1519 80 μ m; L= 120 μ m.

1520 **Figure 9.** ML phylogeny of *Rhipidosiphon*. Bootstraps and Posterior probabilities (bs/PP) are indicated
 1521 at nodes. Species hypotheses obtained using the five species delimitation methods on the two
 1522 markers are shown on the right, along with allocated species names, illustrations and geographical
 1523 distribution (B= *R. sp4*; D= *R. javensis*). The genus symplesiomorphies and synapomorphies, which
 1524 were identified by inferring morphological characters on the time-calibrated phylogeny, are shown
 1525 on the left. Image rights: Payri, C.E.; Lasne, G, Coppejans et al. (2011;*).

1526 **Figure 10.** *Udoteopsis maiottensis* (NOU203562; NOU203570; PC0171655). **A**, Herbarium specimen.
 1527 **B**, Specimen with corticated stipe and growth zone at the margin. **C-E**, Frond. **C**, Smooth siphon;
 1528 asymmetrical dichotomies with constrictions. **D**, Calcified siphons sheath with pores or cracks. **E**,
 1529 Growth zone with swollen siphons. **F-H**, Corticated stipe with protuberances. Scale bars: B= 0.75 cm;
 1530 C= 125 μ m; D= 16 μ m; E= 120 μ m; F= 250 μ m; G= 415 μ m; H= 250 μ m.

1531 **Supporting Information**

1532 **Data S1:** Morpho-anatomical characters studied and associated states.

1533 **Data S2:** Results of the species delimitation analyses on *tufA* and *rbcL* markers.

1534 **Data S3:** Supports (ML) of hPTP partitions for the *tufA* dataset on Udoteaceae.

1535 **Data S4:** Supports (ML) of hPTP partitions for the *rbcL* dataset on Udoteaceae.

1536 **Data S5:** Summary of correlations, ancestral estimations and stochastic mapping results for all the
1537 characters studied.

1538

1539 **Figure S1:** Species delimitation results obtained with the five methods (ABGD, GMYC, bGMYC, PTP
1540 and mPTP) on the *tufA* dataset. The tree represented is MCCT tree from the BEAST analysis.

1541 Partitions retained as SSHs following the majority rule are indicated by black bars. Blue bars
1542 represent the partition retained as SSHs, although not in the majority rule, while grey bars are the
1543 different partitions not retained. The defined SSHs (= clades) are indicated in the right column,
1544 together with species assignments obtained from morpho-anatomical observations.

1545 **Figure S2:** Species delimitation results obtained with the five methods (ABGD, GMYC, bGMYC, PTP
1546 and mPTP) on the *rbcL* dataset. The tree represented is MCCT tree from the BEAST analysis Partitions

1547 retained as SSHs following the majority rule are indicated by black bars. Blue bars represent the
1548 partition retained as SSHs, although not in the majority rule while grey bars are the different
1549 partition not retained. The defined SSHs (= clades) are indicated in the right column, together with
1550 species assignments obtained from morpho-anatomical observations.

1551 **Figure S3:** ML phylogeny of the Udoteaceae obtained using RAXML on chloroplast genes (*tufA+rbcL*).

1552 Bootstraps are indicated at nodes.

1553 **Figure S4:** ML phylogeny of the Udoteaceae obtained using RAXML on the nuclear 18S rDNA gene.
1554 Bootstraps are indicated at nodes.

1555 **Figure S5:** ML phylogeny of the “PRRU complex”. Bootstrap and Posterior probabilities (bs/PP) are
1556 indicated at nodes. Species hypotheses obtained using the five species delimitation methods on the
1557 two markers are presented on the right, along with allocated species names and illustrations. The
1558 epithets of the species are left as used in Guiry & Guiry (2020), but are no longer valid after this
1559 study. The two alternative proposals for taxonomic treatment are proposed on the right, as well as
1560 the symplesiomorphies and synapomorphies of the “single genus” hypothesis, identified by inferring
1561 morphological characters on the time-calibrated phylogeny. Image rights: Payri, C.E., Littler & Littler
1562 (2000; *).

1563 **Figure S6:** ML phylogeny of the “PPR complex”. Bootstrap and Posterior probabilities (bs/PP) are
1564 indicated at nodes. The species hypotheses obtained using the five species delimitation methods on
1565 the two markers are shown on the right, along with allocated species names, illustrations and
1566 geographical distribution. Image rights: Payri, C.E.

1567

1568 **Table S1:** List of specimens with sample ID, species identification, location of sampling, Genbank
1569 accession numbers (or BOLD sequence ID in grey for those not submitted), the sequences used in the
1570 species delimitation approach and the corresponding SSH number, as well as the sequences used in
1571 multilocus and time-calibrated phylogenies.

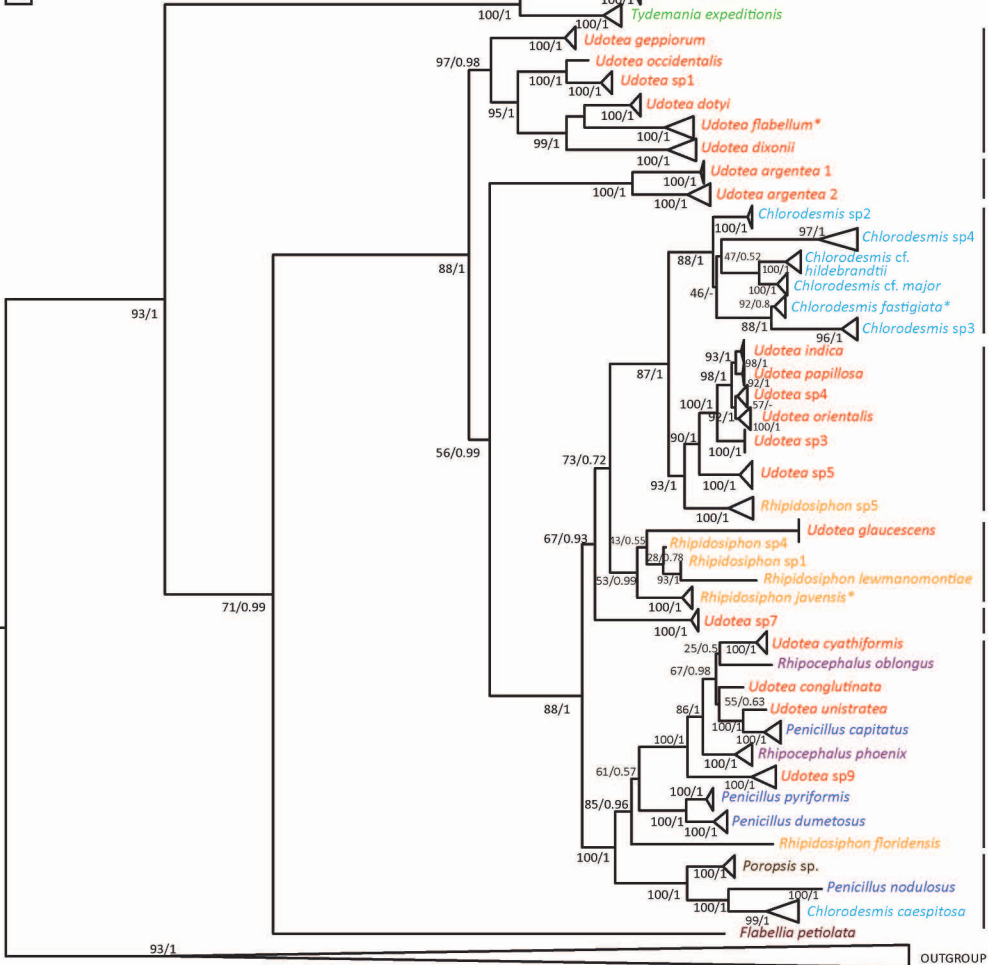
1572 **Table S2:** Primers used for amplification of the *tufA*, *rbcl*, and 18S rDNA markers.

1573 **Table S3:** Details of ML and BI phylogenetic analyses for the different Udoteaceae datasets.

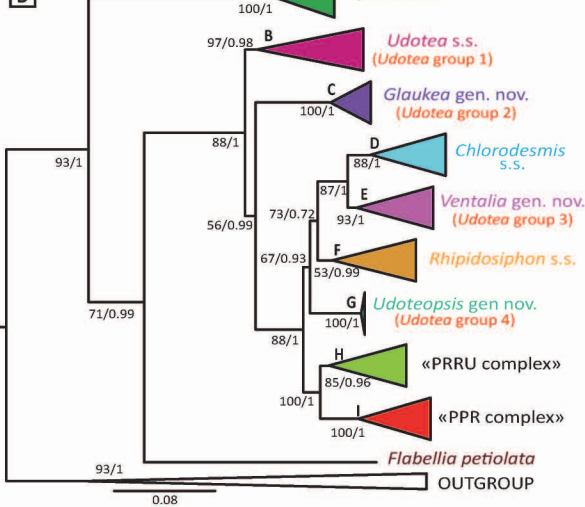
1574 **Table S4:** Calibration points used for the reconstruction of the Udoteaceae time-calibrated
1575 phylogeny. Literature references, age, as well as node position and calibration priors are indicated.

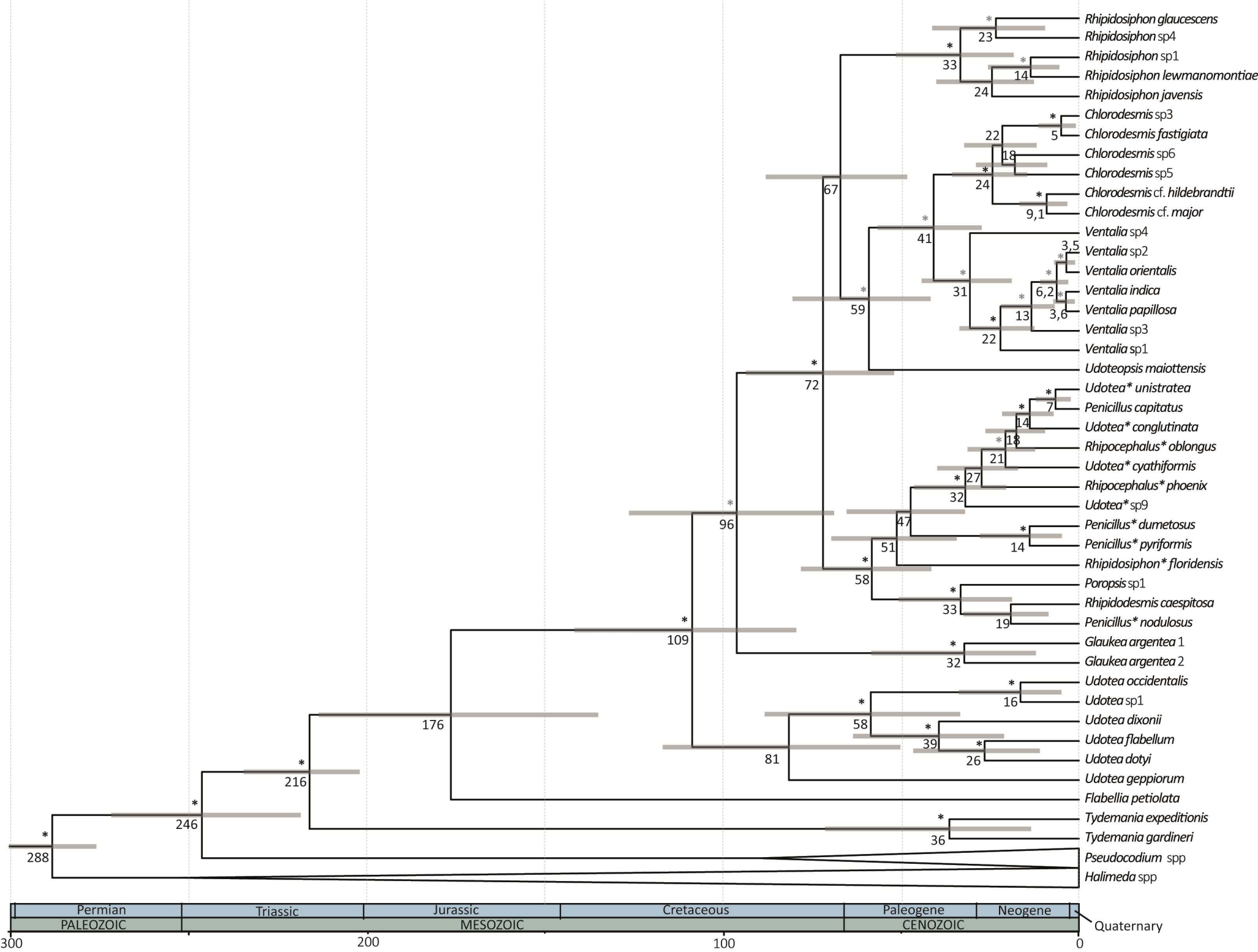
- 1576 **Table S5:** *A posteriori* probabilities (PP) of the partitions defined by the bGMYC method on the *tufA*
1577 marker for Udoteaceae.
- 1578 **Table S6:** *A posteriori* probabilities (PP) of the partitions defined by the bGMYC method on the *rbcL*
1579 marker for Udoteaceae.
- 1580 **Table S7:** Number of common PSHs between the different methods and markers.
- 1581 **Table S8:** Details of the incongruence resolution process and species assignment of the SSHs.
- 1582 **Table S9:** Analysis of the phylogenetic signal (PS) for continuous traits using the Bloomberg (K) and
1583 Pagel statistics (λ). The PS is considered strong if $K > 1$ or $\lambda \geq 1$ and weak if $0 < K < 1$. If $0 < \lambda < 1$, the PS
1584 does not follow the BM model.
- 1585 **Table S10:** Results of phylogenetic signal analyses on discrete characters. Traits with strong
1586 phylogenetic signal ($D < 0$) are indicated in bold with D values in green.
- 1587 **Table S11:** Results of the discrete character correlation test. Acronyms refer to those used in Data S1.
- 1588 **Table S12:** Summary of phylogenetic signal, taxonomic relevance and ancestral state estimation for
1589 each trait studied. The absence of convincing results for a given character is indicated by a "X".

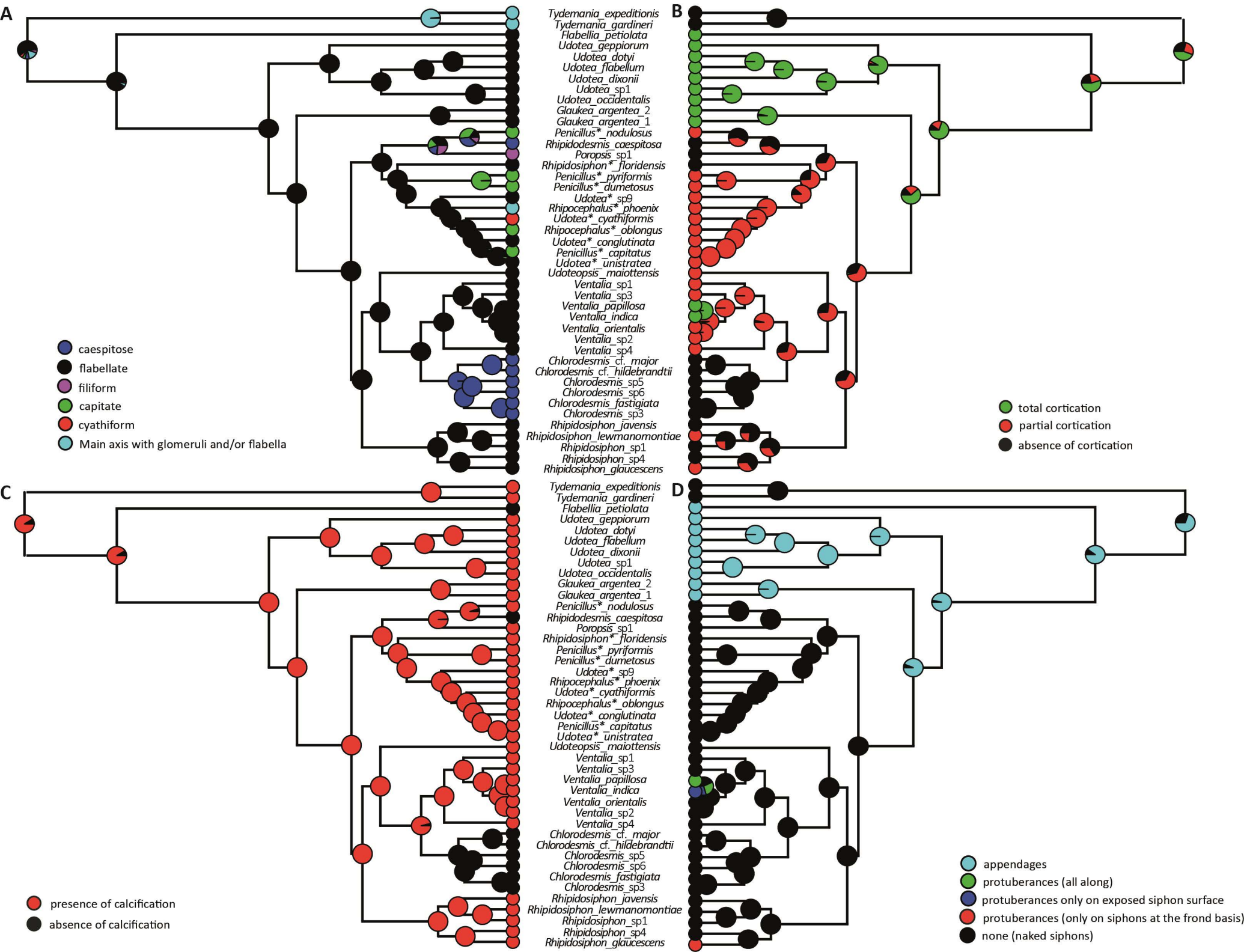
A

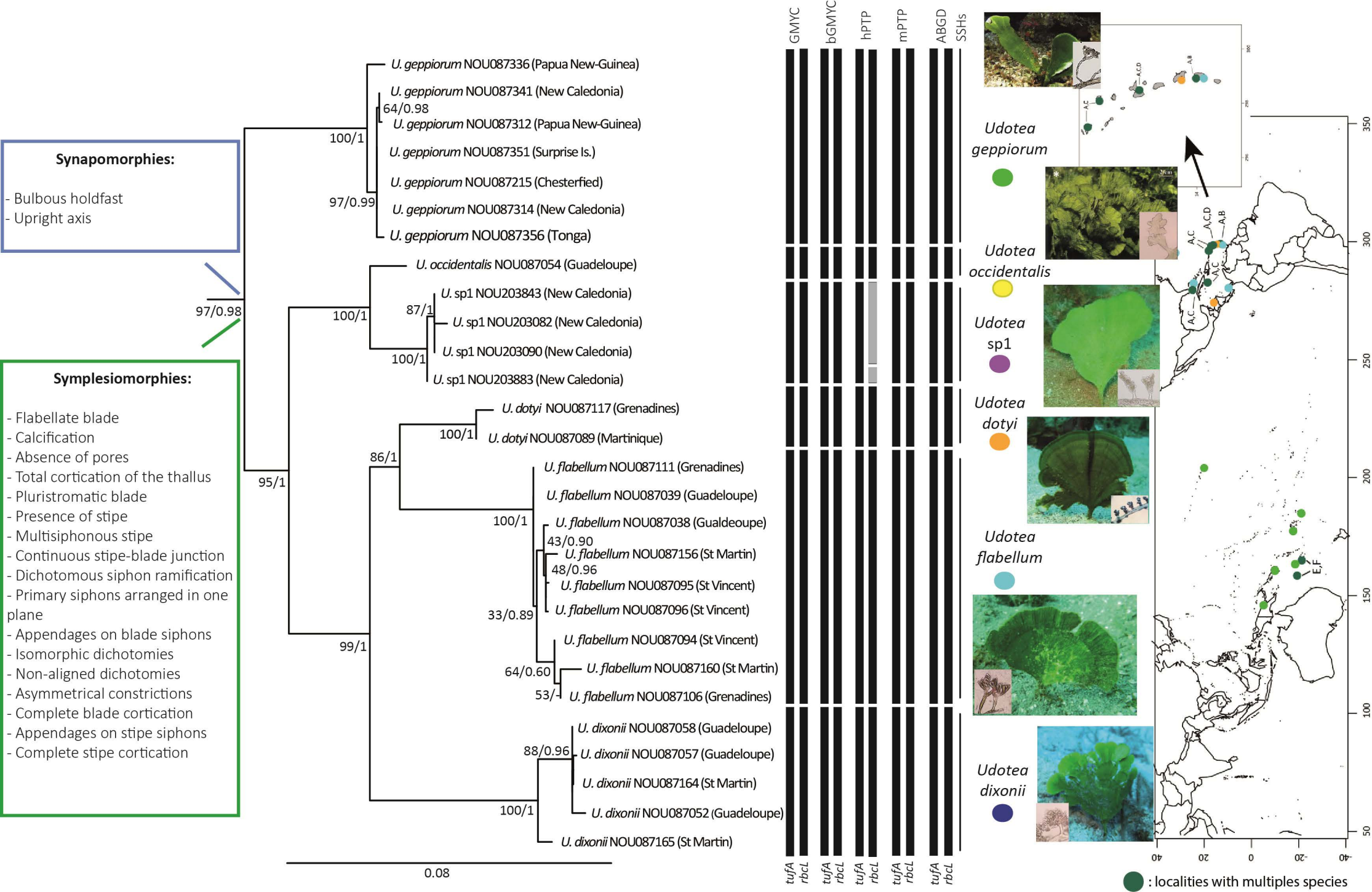


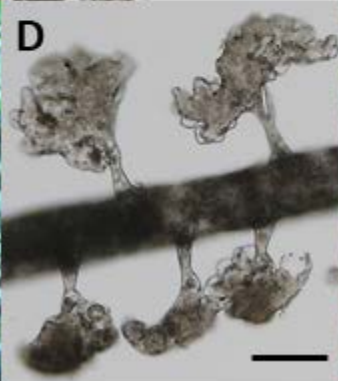
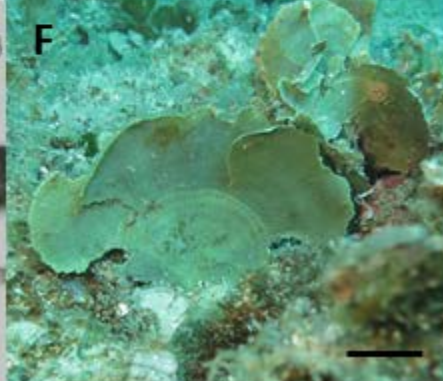
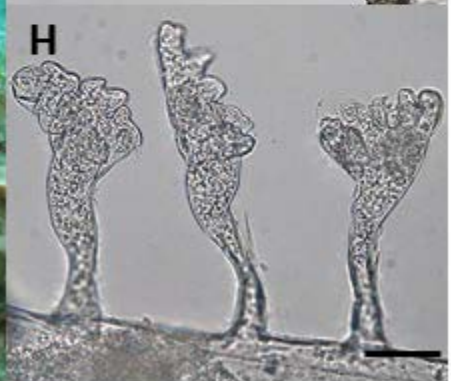
B





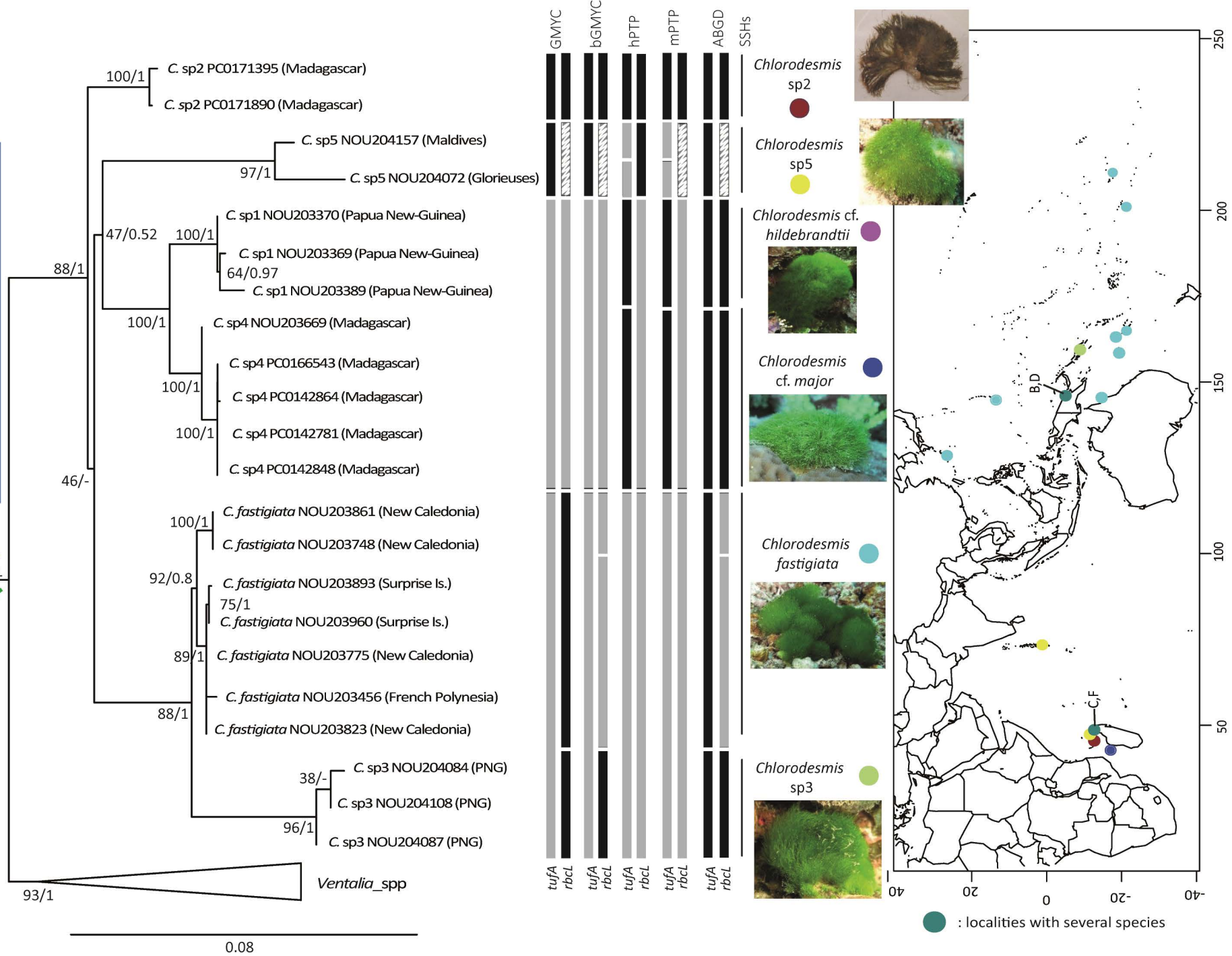


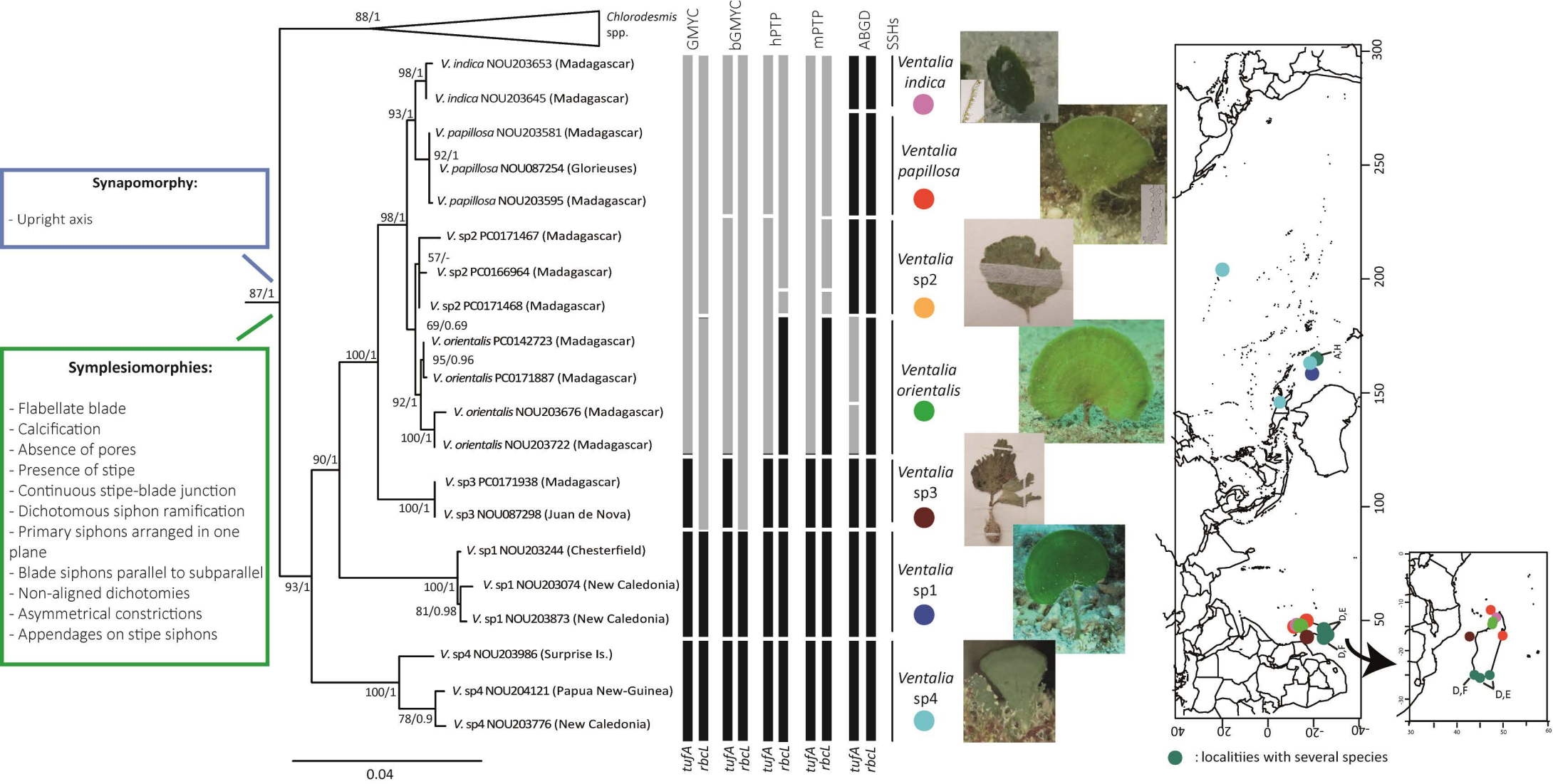


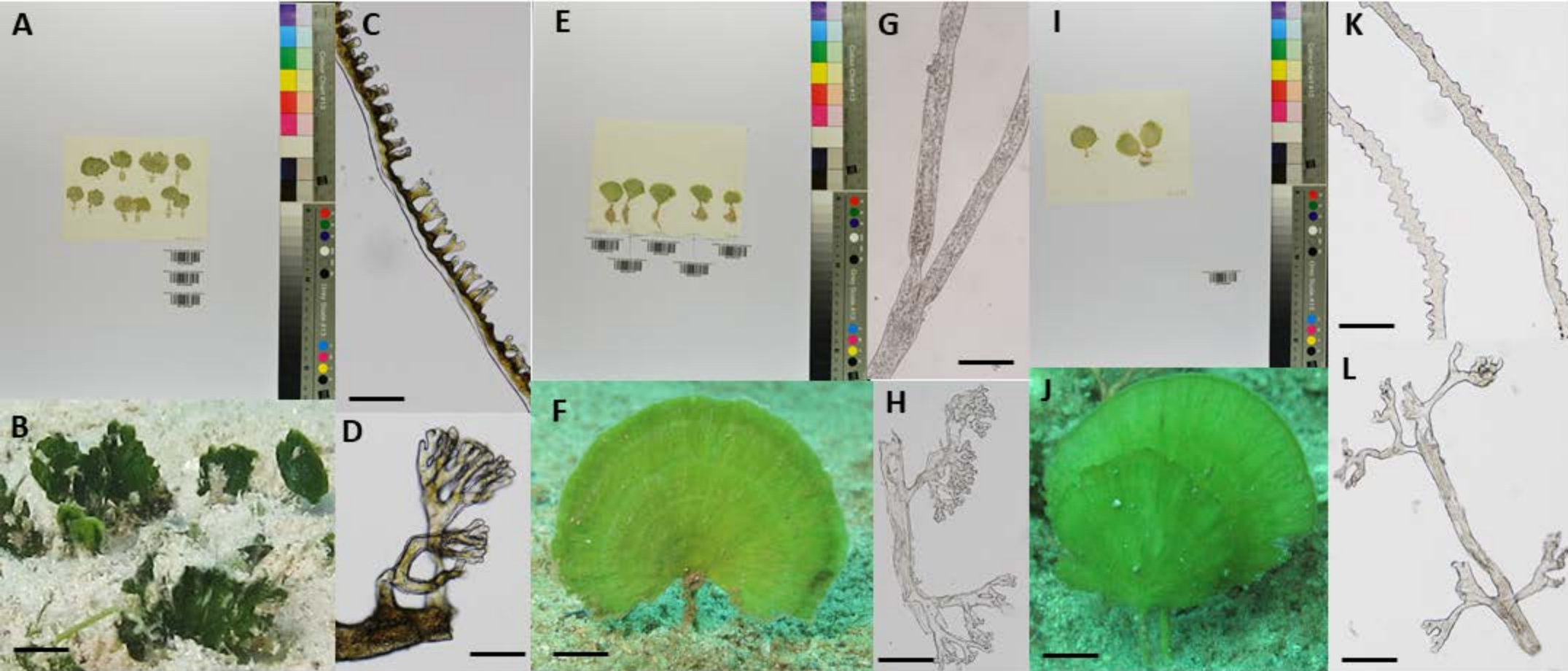
A**C****E****G****B****D****F****H**

- Synapomorphies:**
- Caespitose blade
 - Absence of calcification
 - Absence of thallus cortication
 - Discoid holdfast
 - Absence of stipe
 - Upright axis
 - Interwoven siphons
 - Primary siphons arranged in several planes
 - Absence of secondary structures on blade siphons
 - Absence of blade cortication

- Symplesiomorphies:**
- Unique blade
 - Pluristromatic blade (or in tuft)
 - Dichotomous siphon ramification
 - Presence of supra-dichotomial constrictions





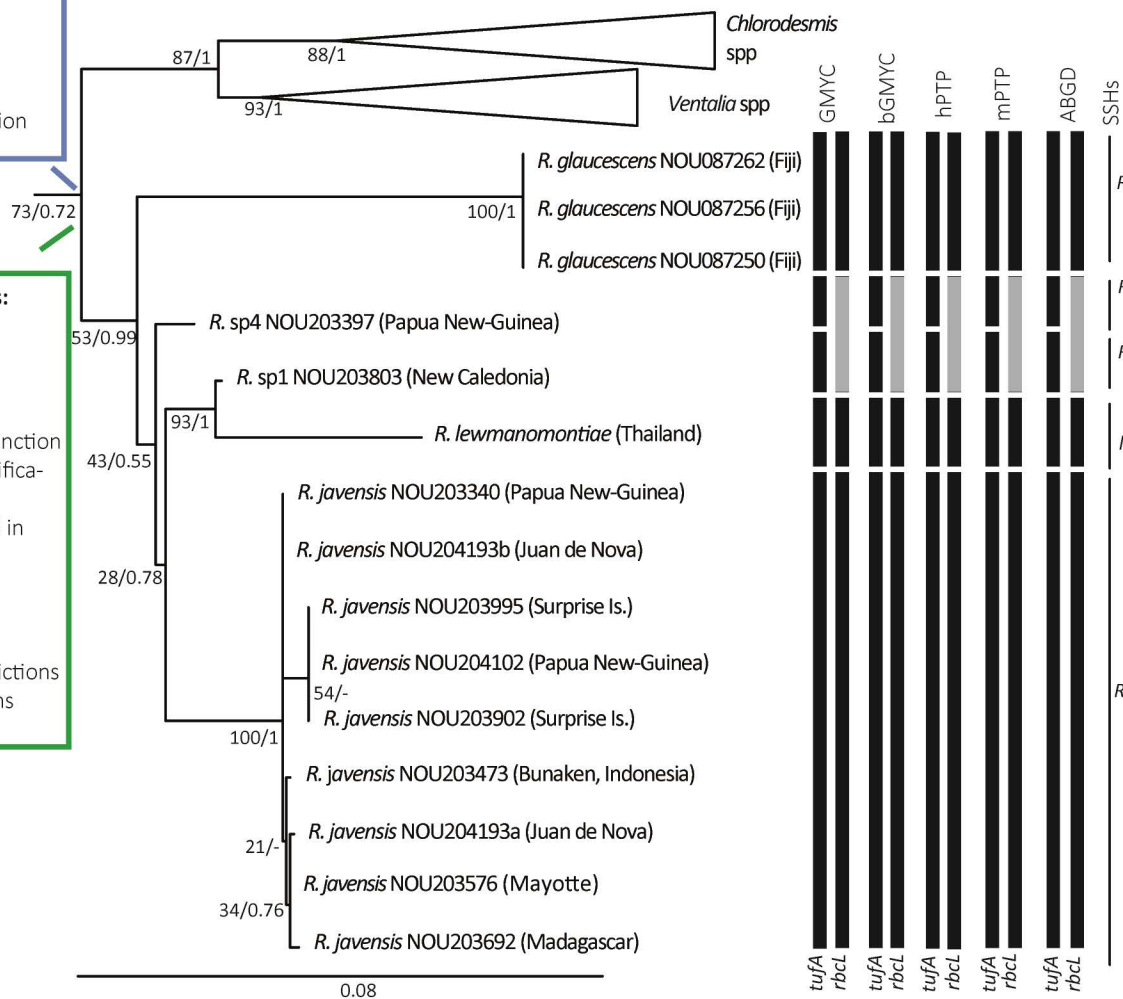


Synapomorphies:

- Monostromatic blade
- Upright axis
- Absence of blade cortication

Symplesiomorphies:

- Flabellate blade
- Calcification
- Presence of stipe
- Continuous stipe-blade junction
- Dichotomous siphon ramification
- Primary siphons arranged in one plane
- Blade siphons parallel to subparallel
- Isomorphic dichotomies
- Supra-dichotomial constrictions
- Asymmetrical constrictions



GMYC

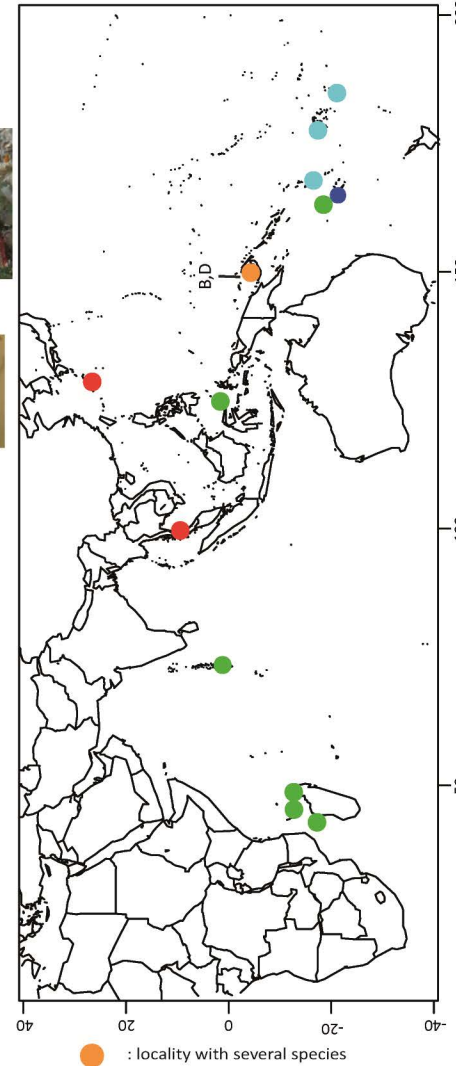
bGMYC

hPTP

mPTP

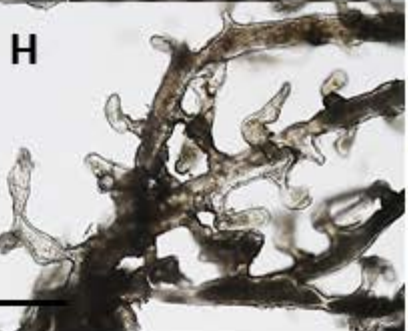
ABGD

SSHs

*Rhipidosiphon glaucescens**Rhipidosiphon sp4**Rhipidosiphon sp1**Rhipidosiphon lewmanomontiae**Rhipidosiphon javensis*

A

RAY 42
leaf of *R. stephanii*

**B****C****D****E****G****H**